Journal of
Mechanics of
Materials and Structures

INELASTIC HEAT FRACTION EVALUATION FOR ENGINEERING PROBLEMS INVOLVING DYNAMIC PLASTIC LOCALIZATION PHENOMENA

Patrice Longère and André Dragon

Volume 4, Nº 2 February 2009

mathematical sciences publishers

JOURNAL OF MECHANICS OF MATERIALS AND STRUCTURES
Vol. 4, No. 2, 2009

INELASTIC HEAT FRACTION EVALUATION FOR ENGINEERING PROBLEMS INVOLVING DYNAMIC PLASTIC LOCALIZATION PHENOMENA

PATRICE LONGÈRE AND ANDRÉ DRAGON

The evaluation of the temperature produced during adiabatic dissipative processes for a large class of engineering materials (metals and some polymers) remains a major subject of interest, notably in the fields of high-speed machining and impact dynamics. The hypothesis consisting in considering the proportion of plastic work dissipated as heat (quantified by the inelastic heat fraction β) as independent on the loading path is now recognized as highly simplistic. Experimental investigations have shown indeed the dependence of the inelastic heat fraction on strain, strain rate and the temperature itself. The theoretical studies available nowadays are not entirely conclusive on various features regarding the history dependence and the evolution of β. The present work attempts to provide a systematic approach to the temperature rise and the inelastic heat fraction evolution for a general loading within the framework of thermoelastic/viscoplastic standard modelling including a number of quantitative variants regarding strain hardening/thermal softening and thermomechanical coupling description. The theoretical results thus obtained are confronted with experimental data from the literature. An analysis of the effects of various model simplifications on the evaluation of temperature growth with regard to conditions for dynamic plastic localization occurrence is also carried out. It is shown that the value of critical shear strain at localization incipience is strongly dependent on the level of simplification admitted.

1. Introduction

As a consequence of dynamic loading under (quasi) adiabatic conditions, many materials, and especially high strength metallic ones, are subject to plastic deformation localization in the form of narrow bands. This phenomenon, known as adiabatic shear banding (ASB), intervenes as thermal softening overcomes strain hardening and is often the precursor of structural failure. Many experimental as well as theoretical studies have been devoted to this deterioration process induced by thermal instability in terms of onset conditions, collective band behaviour and postcritical response [Zener and Hollomon 1944; Recht 1964; Marchand and Duffy 1988; Bai and Bodd 1992; Longère et al. 2005]. They all point out the crucial role of temperature. An accurate knowledge of the heat $\dot{Q}$ generated by the plastic work rate $\dot{W}^p$ during adiabatic dissipative evolution is thus needed. The quantity characterizing the proportion of plastic work dissipated as heat is commonly denoted β, such that $\dot{Q} = \beta \dot{W}^p$, and is usually called the *inelastic heat fraction Taylor–Quinney coefficient* [Taylor and Quinney 1934]. The engineering viewpoint consists in supposing that the inelastic heat fraction coefficient β remains constant during any process. When simulating numerically dynamic adiabatic problems using engineering computation codes, this assumption — which supposes that the coefficient β may be postulated a priori — is useful in the sense that it allows for accounting for thermomechanical couplings without solving the heat equation. In the literature, the value

Keywords: thermomechanics, viscoplasticity, inelastic heat fraction, nonlinear modelling, dynamics, localization.

of β typically ranges from 80 to 100% [Campagne et al. 2005; Guo et al. 2005] — in other words, between 80% or 100% of the plastic work is supposed to be converted into heat. However many experimental investigations have shown that the proportion of plastic work dissipated as heat is strongly dependent on temperature, strain and strain rate. Starting from this crude fact, this paper aims at proposing a more rigorous assessment of the temperature rate $\dot{T}$ and the related inelastic heat fraction coefficient β (as an evolving quantity) for any three-dimensional loading path and thermoelastic/viscoplastic standard materials by using irreversible thermodynamics concepts in the context of adiabatic processes. As an application of this work, the consequences of various levels of simplification for evaluating both of the aforementioned quantities are studied in the context of ASB dynamic plastic localization onset conditions.

According to the extensive review by Bever et al. [1973] concerning the experimental investigations of the ratio a of the stored energy $\dot{W}^s$ to the mechanical energy $\dot{W}$ ($a = \dot{W}^s/\dot{W}$) during various plastic deformation processes, this ratio may be as expected strongly dependent on the loading path, on the material and on the deformation magnitude. In the present work we are rather interested in the energy adiabatically transformed into heat $\dot{Q}$ as a linear function of the plastic deformation energy $\dot{W}^p$ via the so-called inelastic heat fraction β ($\beta = \dot{Q}/\dot{W}^p$). Particularly useful in the numerical simulation of transient problems (crash, shock impact, etc.) for taking into account the thermomechanical coupling under adiabatic conditions without solving the thermal problem, the inelastic heat fraction remains an important subject of investigation, the accuracy of temperature measurement increasing thanks to the improvement of the relevant devices. In this context, some experimental determination of heating during plastic deformation at various strain rates tends to prove the dependence of the inelastic heat fraction on strain, strain rate and temperature [Chrysochoos et al. 1989; Kapoor and Nemat-Nasser 1998; Oliferuk et al. 2004]. Theoretical analyses [Aravas et al. 1990; Zehnder 1991] devoted to the subject agree with the tendency mentioned above but qualitative results appear contradictory [Mason et al. 1994] depending on the basic concepts used. The present work aims to propose an evaluation of the proportion of plastic work dissipated as heat from a broad spectrum of thermoelastic/viscoplastic models within the internal variables framework employing well-established thermodynamic concepts. With this aim in view, and starting from the assumption of the existence of free energy and dissipation potential and applying the first and second principles of thermodynamics, a class of characteristic constitutive three-dimensional thermoelastic/viscoplastic models is investigated with respect to their capacity to reproduce the evolution of β as a function of strain, strain rate and temperature. As the works by Rosakis et al. [2000] for one-dimensional constitutive modelling and Clayton [2005] for crystalline plasticity based modelling, this analysis strives to provide some complementary insight regarding heat generation versus dissipative mechanisms involving strain, strain rate and temperature effects in dynamic plasticity. Comparison of experimental and theoretical results concerning inelastic heat fraction evolution during some simple loading is discussed showing striking effects and paradoxes.

A further item treated in the present work is the analysis of the effects of model simplifications in the evaluation of temperature growth regarding conditions for dynamic plastic localization occurrence. These conditions are obtained from a simplified analysis based on the theory of linear perturbation [Bai 1982; Clifton et al. 1984] in the form of a criterion relating the resolved shear stress to strain hardening, thermal softening and viscosity parameters [Batra and Chen 2001; Longère et al. 2003] in the context of adiabatic shear banding localization. The purpose of the present study is not to discuss or extend the theory but to apply the method in order to obtain a practical criterion reproducing experimental

observation — the reader can refer to [Molinari 1985; Fressengeas and Molinari 1985; Anand et al. 1987] for extensive methodological background. Various levels of simplification of the heat equation formulation are consequently considered yielding corresponding criteria for ASB onset.

In Section 2 selected thermomechanical ingredients are recalled leading to the expression of the heat equation in the case of thermoelastic/viscoplastic modelling. The context considered in this work concerns loading at high strain rates for which adiabatic conditions can be assumed. Dissipative material behaviour is thus supposed to be (visco)plastic and pressure insensitive. The strain rates range considered is typically comprised between 10^2 and $10^4\,\mathrm{s}^{-1}$, and maximum value of temperature remains much lower than the melting point.

In Section 3 several typical material behaviour models are studied including the combined effects of isotropic strain hardening/softening, thermal softening and plastic viscosity. The influence of strain rate and initial temperature as well as the influence of the functions used to describe the aforementioned effects on the temperature rate and on the inelastic heat fraction are shown. A confrontation of the theoretical results with experimental observations available in literature is also discussed.

In Section 4 three levels of simplification of heat equation are studied: first, due to its weak contribution to temperature change the thermoelastic coupling is neglected ; second, thermodissipative couplings are neglected as well ; finally the temperature rise is supposed to be directly linked to the plastic work rate via the inelastic heat fraction assumed to have a constant value. The consequences of these simplifications are examined in the context of thermal instability-induced dynamic plastic localization. With this aim in view, the linear perturbation method is applied to the case of the simple shearing of a volume element consisting of a thermo/viscoplastic material. The further parametric analysis shows how the value of the critical shear strain at localization incipience is strongly dependent on the temperature rise evaluation method.

2. Thermodynamic context and constitutive framework

The irreversible thermodynamics framework is used here to describe the thermoelastic-inelastic response of a material [Perzyna 1966; Bataille and Kestin 1975]. For the first time, expressions of dissipated energy and heat equation are given within the internal variable framework. The different levels of simplification of the heat equation are then introduced in connection with the further study of heat evaluation at the dynamic localization onset.

The instantaneous state of the material is described by a thermodynamic potential, namely the Helmholtz free energy per unit mass $\psi(T, z)$ where T represents absolute temperature — which is supposed to be a well defined entity within the thermodynamic framework employed — and z, a set of normal variables. Gibbs' relation takes the form:

$$\rho_0 \dot{\psi} = -\rho_0 s \dot{T} + Z\dot{z}, \qquad s = -\left.\frac{\partial \psi}{\partial T}\right|_z, \quad Z = \rho_0 \left.\frac{\partial \psi}{\partial z}\right|_T, \tag{1}$$

where ρ_0 represents the mass density in the initial configuration, s the entropy and Z the set of thermodynamic (conjugate) forces associated with the state variables z.

According to the second law of thermodynamics, the mechanical part of dissipated energy is written as

$$D = \boldsymbol{\tau} : \boldsymbol{d} - Z\dot{z} \geq 0, \tag{2}$$

where $\boldsymbol{d}$ represents the rate of deformation tensor and $\boldsymbol{\tau}$ the Kirchhoff stress tensor defined as the Cauchy stress tensor $\boldsymbol{\sigma}$ multiplied by the Jacobian determinant J of the deformation gradient $\boldsymbol{F}$ ($J = \det \boldsymbol{F}$), that is, $\boldsymbol{\tau} = J\boldsymbol{\sigma}$.

Combination of the first law of thermodynamics and of Gibbs relation gives the local form of the heat equation as

$$\rho_0 c_z \dot{T} + J \operatorname{div} \boldsymbol{q} - r = \boldsymbol{\tau} : \boldsymbol{d} - \left(Z - T\frac{\partial Z}{\partial T}\right)\dot{z}, \tag{3}$$

where $\boldsymbol{q}$ is the heat flux vector per unit area, r the heat supply per unit volume, and

$$c_z = -T \left.\frac{\partial^2 \psi}{\partial T^2}\right|_z$$

is the heat capacity at given z.

Equation (3) above relates thermal terms on the left side, including temperature rate $\dot{T}$, heat conduction $\operatorname{div} \boldsymbol{q}$, and heat supply r, to mechanical terms on the right side, including mechanical work rate $\boldsymbol{\tau} : \boldsymbol{d}$ and other work rates $Z\dot{z}$, while the last term $T\partial Z/\partial T\dot{z}$ is referred explicitly to thermomechanical couplings.

The study is now reduced to thermoelastic/viscoplastic behaviour in the case of isotropic strain hardening. The set of state variables is assumed in the form $z \equiv (\boldsymbol{e}^{\mathrm{e}}, p)$, where $\boldsymbol{e}^{\mathrm{e}}$ represents a measure of moderate elastic strain, ($\boldsymbol{e}^{\mathrm{e}} = \ln \boldsymbol{V}^{\mathrm{e}}$; $\boldsymbol{F}^{\mathrm{e}} = \boldsymbol{V}^{\mathrm{e}}\boldsymbol{Q}$ where $\boldsymbol{F}^{\mathrm{e}}$ proceeds from the multiplicative split of the deformation gradient $\boldsymbol{F} = \boldsymbol{F}^{\mathrm{e}}\boldsymbol{F}^{p}$ and where $\boldsymbol{V}^{\mathrm{e}}$ and $\boldsymbol{Q}$ represent the pure elastic stretching and the frame rotation tensors respectively), and

$$p = \int_t \sqrt{\tfrac{2}{3}\,\boldsymbol{d}^p : \boldsymbol{d}^p}\, dt$$

the isotropic strain hardening variable. The set of conjugate forces is thus given in the form $Z \equiv (\boldsymbol{\tau}, R)$, where R represents the isotropic hardening force (affinity).

The rate of deformation (symmetric part of the velocity gradient) $\boldsymbol{d} = [\partial \boldsymbol{v}/\partial \boldsymbol{x}]^S$ is furthermore decomposed into a reversible ('elastic') part

$$\boldsymbol{d}^{\mathrm{e}} = \overset{\nabla}{\boldsymbol{e}}{}^{\mathrm{e}} = \dot{\boldsymbol{e}}^{\mathrm{e}} - \boldsymbol{\omega}\boldsymbol{e}^{\mathrm{e}} + \boldsymbol{e}^{\mathrm{e}}\boldsymbol{\omega},$$

(where ∇ designates the objective Jaumann derivative of a 2nd order tensor) and an irreversible part $\boldsymbol{d}^p$ such that $\boldsymbol{d} = \boldsymbol{d}^{\mathrm{e}} + \boldsymbol{d}^p$ [Sidoroff and Dogui 2001].

The mechanical dissipation in Equation (2) becomes

$$D = \boldsymbol{\tau} : \boldsymbol{d}^p - R\dot{p} \geq 0. \tag{4}$$

The constitutive laws are thus expressed as

$$s = -\left.\frac{\partial \psi}{\partial T}\right|_{\boldsymbol{e}^{\mathrm{e}}, p}, \quad \boldsymbol{\tau} = \rho_0 \left.\frac{\partial \psi}{\partial \boldsymbol{e}^{\mathrm{e}}}\right|_{T,p}, \quad R = \rho_0 \left.\frac{\partial \psi}{\partial p}\right|_{T, \boldsymbol{e}^{\mathrm{e}}}. \tag{5}$$

The free energy density $\psi\,(T, \boldsymbol{e}^{\mathrm{e}}; p)$ is expressed in the form

$$\psi(T, \boldsymbol{e}^{\mathrm{e}}; p) = \psi^{\mathrm{e}}(T, \boldsymbol{e}^{\mathrm{e}}) + \psi^{\mathrm{th}}(T) + \psi^{\mathrm{b}}(T; p), \tag{6}$$

where $\psi^{\mathrm{e}}(T, \boldsymbol{e}^{\mathrm{e}})$ is the recoverable energy including the isotropic linear thermoelasticity, $\psi^{\mathrm{th}}(T)$ is the purely thermal energy, and $\psi^{\mathrm{b}}(T; p)$ is the stored energy, which reflects the competition in the material

between isotropic strain hardening and thermal softening. These contributions are written as

$$\begin{aligned}\rho_0\psi^{\mathrm{e}}(T,\boldsymbol{e}^{\mathrm{e}}) &= \frac{\lambda}{2}(\operatorname{Tr}\boldsymbol{e}^{\mathrm{e}})^2+\mu\boldsymbol{e}^{\mathrm{e}}:\boldsymbol{e}^{\mathrm{e}}-\alpha K(\operatorname{Tr}\boldsymbol{e}^{\mathrm{e}})\vartheta,\\ \rho_0\psi^{\mathrm{th}}(T) &= -\rho_0 c_0\left(T\ln\frac{T}{T_0}-\vartheta\right)-h(0)f(T),\\ \rho_0\psi^{\mathrm{b}}(T,p) &= h(p)f(T)-h(0)f(0),\end{aligned} \tag{7}$$

where λ and μ represent the Lamé elasticity constants, $K=\lambda+\frac{2}{3}\mu$ the bulk modulus, α the thermal dilatation coefficient, c_0 a thermal constant relative to heat capacity, $\vartheta=T-T_0$ the temperature rise, $h(p)$ the stored energy of cold work and $f(T)$ the thermal softening function. For simplification, the thermoelasticity coefficients and c_0 are supposed to be temperature independent.

From now on the elastic deformations will be considered as small (infinitesimal).

After partial derivation of Equation (6) with respect to $(T,\boldsymbol{e}^{\mathrm{e}},p)$, thermodynamic forces $(-s,\boldsymbol{\tau},R)$ are written as

$$-\rho_0 s=-\alpha K\operatorname{Tr}\boldsymbol{e}^{\mathrm{e}}-\rho_0 c_0\ln\frac{T}{T_0}-[h(0)-h(p)]\,f'(T), \tag{8}$$

$$\boldsymbol{\tau}=\left(\lambda\operatorname{Tr}\boldsymbol{e}^{\mathrm{e}}-\alpha K\vartheta\right)\boldsymbol{\delta}+2\mu\boldsymbol{e}^{\mathrm{e}}, \tag{9}$$

$$R=h'(p)f(T). \tag{10}$$

On the other hand, the heat capacity

$$c_z=-T\left.\frac{\partial^2\psi}{\partial T^2}\right|_z=T\left.\frac{\partial s}{\partial T}\right|_z$$

takes the form

$$c_z=c_0+T\frac{[h(0)-h(p)]}{\rho_0}f''(T).$$

Assuming a negligible contribution of the thermoplastic coupling term of this expression (this term is always zero since $f(T)$ is an affine function), the heat capacity is supposed to be constant, that is, $c_z=c_0$.

By rewriting the mechanical dissipation equation (4) in the form $D=\bar{Z}\dot{\bar{z}}\geq 0$, $\bar{Z}=(\boldsymbol{\tau},R)$ represents the set of thermodynamic forces associated to the set of fluxes $\dot{\bar{z}}=\left(\boldsymbol{d}^p,-\dot{p}\right)$. Considering now time-dependent plasticity and applying the normality rule with respect to the dual $\Psi\left(\bar{Z}\right)$ of the dissipation potential, depending on $\bar{Z}$ via the loading (yield) function $F\left(\bar{Z}\right)$ (that is, standard rule for $\dot{\bar{z}}$), internal state variable evolution laws are deduced from:

$$\dot{\bar{z}}=\Lambda\frac{\partial F\left(\bar{Z}\right)}{\partial\bar{Z}},\qquad \Lambda=\frac{\partial\Psi(F)}{\partial F}\geq 0, \tag{11}$$

where Λ represents the viscous multiplier governing dissipative mechanisms of plasticity.

Applying the normality rule to the present case yields

$$\boldsymbol{d}^p=\Lambda\frac{\partial F}{\partial\boldsymbol{\tau}};\qquad -\dot{p}=\Lambda\frac{\partial F}{\partial R}. \tag{12}$$

The yield function $F\left(\bar{Z}\right)$ in Equation (11) is assumed in the form of a Huber–von Mises criterion:

$$F\left(\boldsymbol{\tau}, R; T\right) = J_2\left(\boldsymbol{\tau}\right) - g(R, T), \tag{13}$$

where $J_2\left(\boldsymbol{\tau}\right) = \sqrt{\frac{3}{2}\boldsymbol{s} : \boldsymbol{s}}$ and $\boldsymbol{s} = \boldsymbol{\tau} - \frac{\mathrm{Tr}\,\boldsymbol{\tau}}{3}\,\boldsymbol{\delta}$ represents the stress deviator tensor.

The strain hardening function $g(R, T)$ in Equation (13) representing the Huber–von Mises surface radius is expressed by

$$g(R, T) = R_0 f(T) + R(T, p). \tag{14}$$

Evolution laws in Equation (12) are thus detailed as

$$\boldsymbol{d}^p = \frac{3}{2}\Lambda\frac{\boldsymbol{s}}{J_2}; \qquad \dot{p} = \Lambda. \tag{15}$$

The model is completed by the expression of the force potential in (11):

$$\Psi(F) = \frac{Y}{m+1}\left\langle\frac{F}{Y}\right\rangle^{m+1}, \qquad \Lambda = \left\langle\frac{F}{Y}\right\rangle^{m} = H(F). \tag{16}$$

Inverting Equation $(16)_2$ and using (13), (14) and (15) yield

$$J_2 = R_0 f(T) + R(T, p) + \Phi\left(T, p, \dot{p}\right) \tag{17}$$

with $\Phi = H^{-1}$. According to Equation $(15)_{1,2}$, the rate of plastic work $\boldsymbol{\tau} : \boldsymbol{d}^p$ in (4) is thus given by:

$$\boldsymbol{\tau} : \boldsymbol{d}^p = J_2\dot{p} = \left[R_0 f(T) + R(T, p) + \Phi\left(T, p, \dot{p}\right)\right]\dot{p}. \tag{18}$$

Furthermore Equation (3) becomes

$$\rho_0 c_0\dot{T} + J\,\mathrm{div}\,\boldsymbol{q} - r = \boldsymbol{\tau} : \boldsymbol{d}^p + T\frac{\partial\boldsymbol{\tau}}{\partial T} : \boldsymbol{d}^{\mathrm{e}} - \left(R - T\frac{\partial R}{\partial T}\right)\dot{p}. \tag{19}$$

The context considered here concerns loading at high strain rate excluding heat supply and for which conditions can be assumed as adiabatic (dynamic loading). Relation (19) is thus reduced to

$$\rho_0 c_0\dot{T} = \boldsymbol{\tau} : \boldsymbol{d}^p + T\frac{\partial\boldsymbol{\tau}}{\partial T} : \boldsymbol{d}^{\mathrm{e}} - \left(R - T\frac{\partial R}{\partial T}\right)\dot{p}. \tag{20}$$

In Equation (20), $\boldsymbol{\tau} : \boldsymbol{d}^p$ represents the plastic part of the mechanical work rate (plastic work rate), $R\dot{p}$ the stored energy rate (the difference $\boldsymbol{\tau} : \boldsymbol{d}^p - R\dot{p}$ represents the unrecoverable energy rate dissipated by heating; see Equation (4)) , $T\left(\partial\boldsymbol{\tau}/\partial T\right) : \boldsymbol{d}^{\mathrm{e}}$ the thermoelastic coupling contribution which describes cooling during a tensile loading and heating during a compressive one, and $T\left(\partial R/\partial T\right)\dot{p}$ the thermoplastic coupling contribution which expresses the stored energy release rate during the temperature rise (see [Clayton 2005] for a similar approach).

In the following, the effects of strain hardening and thermal softening (acting both on isotropic hardening force) on temperature rise are studied. Thermoelastic coupling contribution to temperature rise is actually particularly significant in problems involving very high velocity impact and/or high pressure shock loading. In the context of this work, velocity and pressure are considered moderate and thermoelastic coupling is neglected.

Accounting for Equation (18), relation (20) is thus reduced to

$$\dot{T} = \frac{1}{\rho_0 c_0}\left[J_2 - \left(R - T\frac{\partial R}{\partial T}\right)\right]\dot{p}. \tag{21}$$

Injecting the expression (17) of the stress invariant J_2 and the expression (10) for R yields

$$\dot{T} = \frac{R_0 f(T) + T h'(p) f'(T) + \Phi(T, p, \dot{p})}{\rho_0 c_0}\dot{p}. \tag{22}$$

Remark 1. Comparing the dissipation form in Equations (4) and (22) yields

$$\rho_0 c_0 \dot{T} = D + T h'(p) f'(T)\dot{p}. \tag{23}$$

The dissipation is positive while the second term on the right side is negative (f' being negative for thermal softening material). The temperature increases if the dissipation is high enough to exceed the thermomechanical coupling term which proceeds from $T\,(\partial R/\partial T)\,\dot{p}$ in Equation (21). The condition for temperature growth is written from (23) as

$$R_0 f(T) + \Phi(T, p, \dot{p}) > T h'(p) f'(T). \tag{24}$$

For $R_0 = 0$, there is thus a competition between viscous and thermomechanical effects regarding temperature changes. Neglecting this last contribution leads to the common relation

$$\rho_0 c_0 \dot{T} = D. \tag{25}$$

Furthermore, starting from the definition of the inelastic heat fraction β as $\beta = \rho_0 c_y \dot{T}/\boldsymbol{\tau} : \boldsymbol{d}^p$ and under the aforementioned assumptions, the following expression is deduced from (21):

$$\beta = 1 - \frac{R - T\frac{\partial R}{\partial T}}{J_2}. \tag{26}$$

Injecting the complete expressions of J_2 and R from (17) and (10) gives

$$\beta = 1 - \frac{h'(p)\left[f(T) - T f'(T)\right]}{\left[R_0 + H'(p)\right] f(T) + \Phi(T, p, \dot{p})}. \tag{27}$$

Consequently the inelastic heat fraction β is explicitly a function of temperature, strain and strain rate. Starting from relation (27), a series of comments can be made.

Remark 2. For cumulated plastic strain $p_2 > p_1$ close enough to consider that $T_1 \approx T_2 \approx T$, one can write from (27):

$$\beta(T, p_2, \dot{p}) - \beta(T, p_1, \dot{p}) \approx -\left[h'(p_2) - h'(p_1)\right]\frac{f(T) - T f'(T)}{\left[R_0 + h'(p)\right] f(T) + \Phi(T, p, \dot{p})}. \tag{28}$$

Using the notation

$$\chi = \frac{f(T) - T f'(T)}{\left[R_0 + h'(p)\right] f(T) + \Phi(T, p, \dot{p})}, \tag{29}$$

with $\chi > 0$ as long as $f(T) - Tf'(T) > 0$, which is the case for most (thermal softening) materials, relation (28) is reduced to

$$\frac{\partial \beta}{\partial p} \approx -\chi h''(p). \tag{30}$$

According to (30), it is possible to conclude that for a material exhibiting strain hardening ($h''(p) > 0$), the inelastic heat fraction is decreasing for increasing strain, that is, $\partial\beta/\partial p < 0$. Oppositely, for material exhibiting strain softening ($h''(p) < 0$), the inelastic heat fraction is increasing for increasing strain, that is, $\partial\beta/\partial p > 0$.

Remark 3. According to (27), $\beta(T, p, \dot{p})$ is equal to unity when $h'(p)[f(T) - Tf'(T)] = 0$ which is satisfied for a perfectly plastic material ($h'(p) = 0$) or for a material exhibiting a linear dependence of strain hardening on temperature ($f(T) = AT$). Finally, $\beta = 1$ for any loading path allowing for $f(T) = Tf'(T)$.

Remark 4. Suppose now that $f(T_0) = \varsigma$ $(0 < \varsigma < 1)$, $f'(T_0) = -\xi$ $(\xi > 0)$, and let us note that $h'(0) = R_1 > 0$.

In this case, according to (27),

$$\beta_0 = \beta(T_0, 0, \dot{p}) = 1 - \frac{R_1(\varsigma + \xi T_0)}{(R_0 + R_1)\varsigma + \Phi(T_0, 0, \dot{p})},$$

and for any $R_1 \neq 0$, one obtains $\beta_0 < 1$.

Remark 5. Suppose finally that $f(T) = 1 - AT$ $(A > 0)$, $R_0 = 0$ and $\Phi(T, p, \dot{p}) = h'(p) f(T) z(\dot{p})$.

In this case

$$\beta(T, p, \dot{p}) = 1 - \frac{1}{f(T)[1 + z(\dot{p})]} = \beta(T, \dot{p}).$$

Thus β does not depend on the plastic strain p. On the other hand, for a given strain rate $\dot{p}$, as $f(T)$ decreases with increasing temperature T, then β decreases with increasing temperature, and for a given temperature T, as $z(\dot{p})$ increases with increasing strain rate $\dot{p}$, then β increases with increasing strain rate $\dot{p}$.

By employing the inelastic heat fraction considered as a constant, heat equation is reduced to

$$\dot{T} = \frac{\beta}{\rho_0 c_0} J_2 \dot{p}. \tag{31}$$

Injecting (17) into (31) yields

$$\dot{T} = \beta \frac{\left[R_0 + h'(p)\right] f(T) + \Phi(T, p, \dot{p})}{\rho_0 c_0} \dot{p}. \tag{32}$$

Expression (32) above has to be compared with expression (22). In particular, the temperature rate here is always positive (see Remark 1).

3. Application to usual models

Following conventional experimental procedures, material constants for most models are identified from a series of tests carried out at various strain rates for a given initial temperature and/or at different temperatures for a given nominal (generally low) strain rate. In this context, the respective contributions

of separated effects of temperature, strain and strain rate can be determined during the material constant numerical identification. The latter needs, for high strain rate (adiabatic) tests, the evaluation of heating produced by the plastic work, that is, an expression for the inelastic heat fraction.

In this section, various thermodynamic and/or engineering models are studied in terms of stress invariant, temperature and inelastic heat fraction evolutions. Independently of the genuine temperature evolution in the material, the influence of the choice of the model is pointed out. As usually assumed, adiabatic conditions are supposed to prevail at strain rates higher than $100\,\mathrm{s}^{-1}$.

According to the methodology detailed previously, a series of mathematical functions available in literature has been selected and reported in the following tables.

Tables 1–3 give the usual functions describing the effects of strain hardening/softening, thermal softening and strain rate, respectively. Corresponding abbreviations used later in the analysis are also given.

The Ramberg–Osgood (HRO) model in Table 1 for strain hardening has the form of a power law. For $n = 0$, stored energy is linear (HL with $\mathrm{HL} = \mathrm{HRO}_{n=0}$) with respect to cumulated plastic strain while the material is perfectly plastic; for $n = 1$, stored energy evolves as a quadratic function (HQ with

	Ramberg–Osgood HRO	Voce HV	Strain softening HS
$h(p)$	$k\dfrac{p^{n+1}}{n+1}$	$R_\infty[p+\dfrac{1}{k}\exp(-kp)]$	$-\dfrac{R_\infty}{k}\exp(-kp)$
$h'(p)$	kp^n	$R_\infty[1-\exp(-kp)]$	$R_\infty\exp(-kp)$
$h''(p)$	nkp^{n-1}	$kR_\infty\exp(-kp)$	$-kR_\infty\exp(-kp)$

Table 1. Usual strain hardening/softening functions $h(p)$.

	Linear FL	Power FP	Exponential FE
$f(T)$	$1-AT$	$1-\left(\dfrac{T-T_r}{T_m-T_r}\right)^m$	$\exp(-\gamma T)$
$f'(T)$	$A>0$	$-\dfrac{m}{T_m-T_r}\left(\dfrac{T-T_r}{T_m-T_r}\right)^{m-1}$	$-\gamma\,.\exp(-\gamma T)$
$f''(T)$	0	$\dfrac{m(1-m)}{(T_m-T_r)^2}\left(\dfrac{T-T_r}{T_m-T_r}\right)^{m-2}$	$\gamma^2\exp(-\gamma T)$

Table 2. Usual thermal softening functions $f(T)$.

	additive type ADD	multiplicative type MUL	Exponential type EXP
$\dot p = H\langle F\rangle$	$1/\tau_0\langle F/R_0\rangle^m$	$1/\tau_0\langle F/R\rangle^m$	$\dot p_0\exp\langle F/CR\rangle$
τ_0	$\langle Y/R_0\rangle^m$	τ_0	$1/\dot p_0$
$\Phi = H^{-1}$	$Y\dot p^{1/m}$	$R\tau_0^{1/m}\dot p^{1/m}$	$CR\ln(\dot p/\dot p_0)$

Table 3. Usual strain rate functions $H\langle F\rangle$.

$\mathrm{HQ} = \mathrm{HRO}_{n=1}$) of cumulated plastic strain and hardening is linear with respect to cumulated plastic strain; for most metals the value of n is comprised between 0 and 1. The Voce (HV) model describes strain hardening with saturation stress, the latter being represented by R_∞. Finally, the strain softening model (HS) is retained in this study as an exponential decreasing function. On the other hand, the combination of several strain hardening/softening functions is designated by linking corresponding abbreviations. HMLRO designates, for example, hardening/softening behaviour (H) described using multiple (M) functions including linear hardening (L) and Ramberg–Osgood (RO). HMSQ designates hardening/softening behaviour (H) described using multiple (M) functions including softening (S) and the quadratic hardening Ramberg–Osgood (Q) function.

The linear function (FL) in Table 2 for thermal softening can be considered as an approximation, for low temperature changes, of a more complex dependence of material behaviour on temperature. The power law (FP) accounts for melting point T_m and room temperature T_r in a power law expression as proposed notably by Johnson and Cook [1983]. Finally a third thermal model (FE) is proposed in the form of an exponential decreasing function which is valid in a wider range of temperature variations than linear function (FL).

The additive type (ADD) and multiplicative type (MUL) functions in Table 3 are used to describe phenomenologically the effects of plastic viscosity in bcc/hcp and fcc metals respectively. The origin of the exponential type function (EXP) proceeds from physical considerations including the concept of thermally activated plastic deformation mechanism.

In the multiplicative type (MUL) in Table 3, the strain rate function

$$\Phi\left(T, p, \dot{p}\right) = R\tau_0^{1/m}\dot{p}^{1/m}$$

can be rewritten in the form

$$\Phi\left(T, p, \dot{p}\right) = h'(p)f(T)g\left(\dot{p}\right),$$

where $g\left(\dot{p}\right) = \tau_0^{1/m}\dot{p}^{1/m}$. In the same way, in the exponential type (EXP) in Table 3, the strain rate function

$$\Phi\left(T, p, \dot{p}\right) = CR\ln\left(\dot{p}/\dot{p}_0\right)$$

can be rewritten in the form

$$\Phi\left(T, p, \dot{p}\right) = h'(p)f(T)g\left(\dot{p}\right),$$

where $g\left(\dot{p}\right) = C\ln\left(\dot{p}/\dot{p}_0\right)$. These expressions may illustrate Remark 5.

Table 4 gives the abbreviations corresponding to models with or without initial yield stress, that is, an initial (or no) nonzero value for the radius of the Huber–von Mises surface, see (14). Note that this concept of initial yield stress may be entirely contained in the state potential (free energy) through a contribution attributed to residual stresses induced by thermomechanical processes and described via a quadratic strain hardening (HRO type model with n=1; see Table 1). As shown previously, the retained viewpoint (nonzero value for the initial radius of the Huber–von Mises surface or residual stresses) is not without consequence for heat evaluation (see (22) and Remark 1).

Remark 6. Consider the combination HL-FE-WYS (see Tables 1, 2 and 4 with $\mathrm{HL} = \mathrm{HRO}_{n=0}$) such that $\rho_0\psi^{\mathrm{b}} = R_1 p\exp\left(-\gamma T\right)$. The yield function is written as

$$F = J_2\left(\boldsymbol{\sigma}\right) - \left[R_0\exp\left(-\gamma T\right) + R\right].$$

With initial yield stress WYS	Without initial yield stress NYS
$R_0 f(T)$	0

Table 4. Existence of initial yield stress.

The strain hardening force and its derivative with respect to temperature are, respectively,

$$R = \rho_0 \partial \psi^{\mathrm{b}} / \partial p = R_1 \exp(-\gamma T), \qquad T \partial R / \partial T = -\gamma T R.$$

In this case, $f(T_0) = \exp(-\gamma T_0) > 0$ and $f'(T_0) = -\gamma \exp(-\gamma T_0)$. As mentioned in Remark 4, the initial inelastic heat fraction β_0 is lower than unity.

In order to analyse the three-dimensional constitutive models built from the combination of strain hardening and thermal softening functions in Tables 1–4, the loading path considered here is the simple shearing. Designate by $\boldsymbol{l} = \partial \boldsymbol{v} / \partial \boldsymbol{x}$ the velocity gradient tensor and l_{ij} its components. We are considering here the simple shear loading such that $v_1 = \dot{\Gamma} x_2$. In this case, the components of the velocity gradient tensor $\boldsymbol{l}$ are zero except $l_{12} = \partial v_1 / \partial x_2 = \dot{\Gamma} \neq 0$.

A set of thermoelastic/viscoplastic models has been tested including various forms for strain hardening, strain softening and their combinations. They all use the physical material constants reported in Table 5.

Evolution of the second invariant of the stress-deviator J_2, temperature T and inelastic heat fraction β is given versus shear strain $e_{12} = \gamma_{12}/2$ (the strain tensor $\boldsymbol{e}$ is obtained by time integration of the nonobjective strain rate tensor $\dot{\boldsymbol{e}}$, with $\dot{\boldsymbol{e}} = \boldsymbol{d} + \boldsymbol{\omega e} - \boldsymbol{e\omega}$) at various strain rates $\dot{\Gamma}$ and initial temperatures T_0 in Figures 1–5 for several models including strain hardening/softening, thermal softening and viscous effects. Adiabatic conditions are assumed for strain rates higher than 100 s^{-1}.

The physical feature of the numerical results obtained is further discussed in Section 3.1 by considering experimental data from literature.

3.1. ***Strain hardening models.*** Consider the combination HV-FL-ADD-WYS (see Tables 1–4) summarized in Table 6. As mentioned before, this combination may correspond to a bcc metal with saturating strain hardening and linear approximation of temperature dependence (Figure 1), such as a high strength martensitic steel.

Figure 1a shows the thermal softening induced under adiabatic conditions for simulations at different plastic strain rates higher than 100 s^{-1}. Figure 1b shows that the temperature rate is higher for higher strain rate, while Figure 1e shows that the temperature rate is lower for higher initial temperature. At 1000 s^{-1} and for $T_0 = 300$ K, the maximal value of temperature increase is close to 60 K.

According to Figure 1c–f, the initial value of β is equal to 1 whatever the strain rate and the initial temperature. At large strain β converges to a value which depends on strain rate and initial temperature with a rate (negative according to Remark 3) whose absolute value increases with decreasing strain

E (GPa)	ν	ρ_0 (kg/m^3)	c_0 (J/kg.K)	α (K^{-1})
200	0,33	7800	420	10^{-6}

Table 5. Physical steel like material constants.

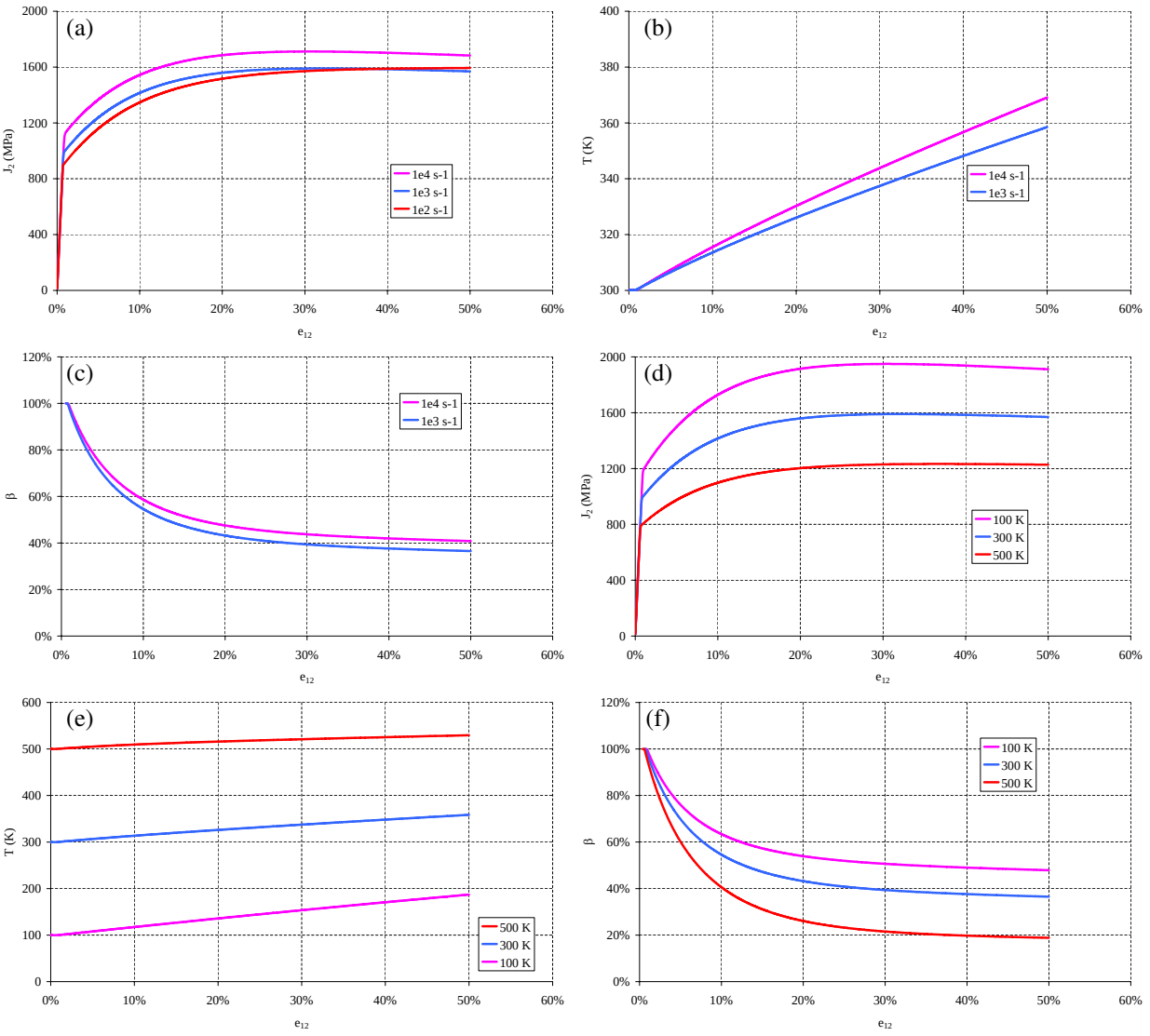

Figure 1. Influence of shear strain rate $\dot{\Gamma}$ and initial temperatures T_0 on stress invariant, heating and inelastic heat fraction for the HV-FL-ADD-WYS hardening model: (a) stress invariant J_2 versus strain e_{12}, with $T_0 = 300\,\mathrm{K}$; (b) temperature T versus strain e_{12}, with $T_0 = 300\,\mathrm{K}$; (c) inelastic heat fraction β versus strain e_{12}, with $T_0 = 300\,\mathrm{K}$; (d) stress invariant J_2 versus strain e_{12}, with $\dot{\Gamma} = 10^3\,\mathrm{s}^{-1}$; (e) temperature T versus strain e_{12}, with $\dot{\Gamma} = 10^3\,\mathrm{s}^{-1}$; (f) inelastic heat fraction β versus strain e_{12}, with $\dot{\Gamma} = 10^3\,\mathrm{s}^{-1}$.

rate and increasing initial temperature. In other words, β depends explicitly on strain, strain rate and temperature.

Consider next the combination HMLRO-FE-MUL-NYS (see Tables 1–4) summarized in Table 7. This combination may correspond to a fcc metal with a power law strain hardening ($n = 0.5$) and exponential dependence on temperature (Figure 2), such as an austenitic steel or a pure copper.

$h(p)$	$f(T)$	$\Phi(T, p, \dot{p})$	R_0
$R_\infty\left[p+\frac{1}{k}\exp(-kp)\right]$	$1-AT$	$Y\dot{p}^{1/m}$	$R_2(1-AT)$

R_∞ (MPa)	k	$A(K^{-1})$	R_2 (MPa)	Y (MPa s$^{1/m}$)	m
1000	20	10^{-3}	1000	100	6

Table 6. Thermoviscoplastic material constants for HV-FL-ADD-WYS model.

In contrast to the previous case, the thermal softening induced under adiabatic conditions for simulations at plastic strain rates greater than 100 s^{-1} does not seem to be really significant (see Figure 2a). In fact, adiabatic thermal effects are present but they are here not able to compensate for strain and strain rate hardening. Figure 2b shows that the temperature rate is higher for higher strain rate while Figure 2e shows that the temperature rate is lower for higher initial temperature. At 1000 s^{-1} and for $T_0 = 300$ K, the maximal value of temperature increase is close to 28 K.

According to Figure 2c–f, the initial value of β is much lower than 1, increasing with increasing strain rate and with decreasing initial temperature. As expected (see Remark 5), the rate of β is close to zero — β does not depend explicitly on strain.

Consider finally the Johnson–Cook engineering model [Johnson and Cook 1983] as the combination HMLRO-FP-EXP-NYS (see Tables 1–4) summarized in Table 8. This model, supposed to describe any metal behaviour, is mainly employed in numerical simulations involving very high strain rates as encountered notably in plate impact and shock.

In Figure 3a the thermal softening induced under adiabatic conditions for simulations at plastic strain rates higher than 100 s^{-1} is not really significant. The temperature rate is seen to be higher for higher

$h(p)$	$f(T)$	$\Phi(T, p, \dot{p})$	R_0	R_1 (MPa)	k	n	γ (K^{-1})	τ_0 (s)	m
$R_1 p + k\frac{p^{n+1}}{n+1}$	$\exp(-\gamma T)$	$R\tau_0^{1/m}\dot{p}^{1/m}$	0	500	1500	0.5	10^{-3}	10^{-4}	10

Table 7. Thermoviscoplastic material constants for HMLRO-FE-MUL-NYS model.

$h(p)$	$f(T)$	$\Phi(T, p, \dot{p})$	R_0
$R_1 p + k(p^{n+1}/n+1)$	$1-\left(\frac{T-T_r}{T_f-T_r}\right)^m$	$CR\ln\frac{\dot{p}}{\dot{p}_0}$	0

R_1 (MPa)	k (MPa)	n	$T_f(K)$	$T_r(K)$	m	$\dot{p}_0$(s^{-1})	C
600	1000	0.3	1800	100	1	1	0,05

Table 8. Thermoviscoplastic material constants for Johnson–Cook model.

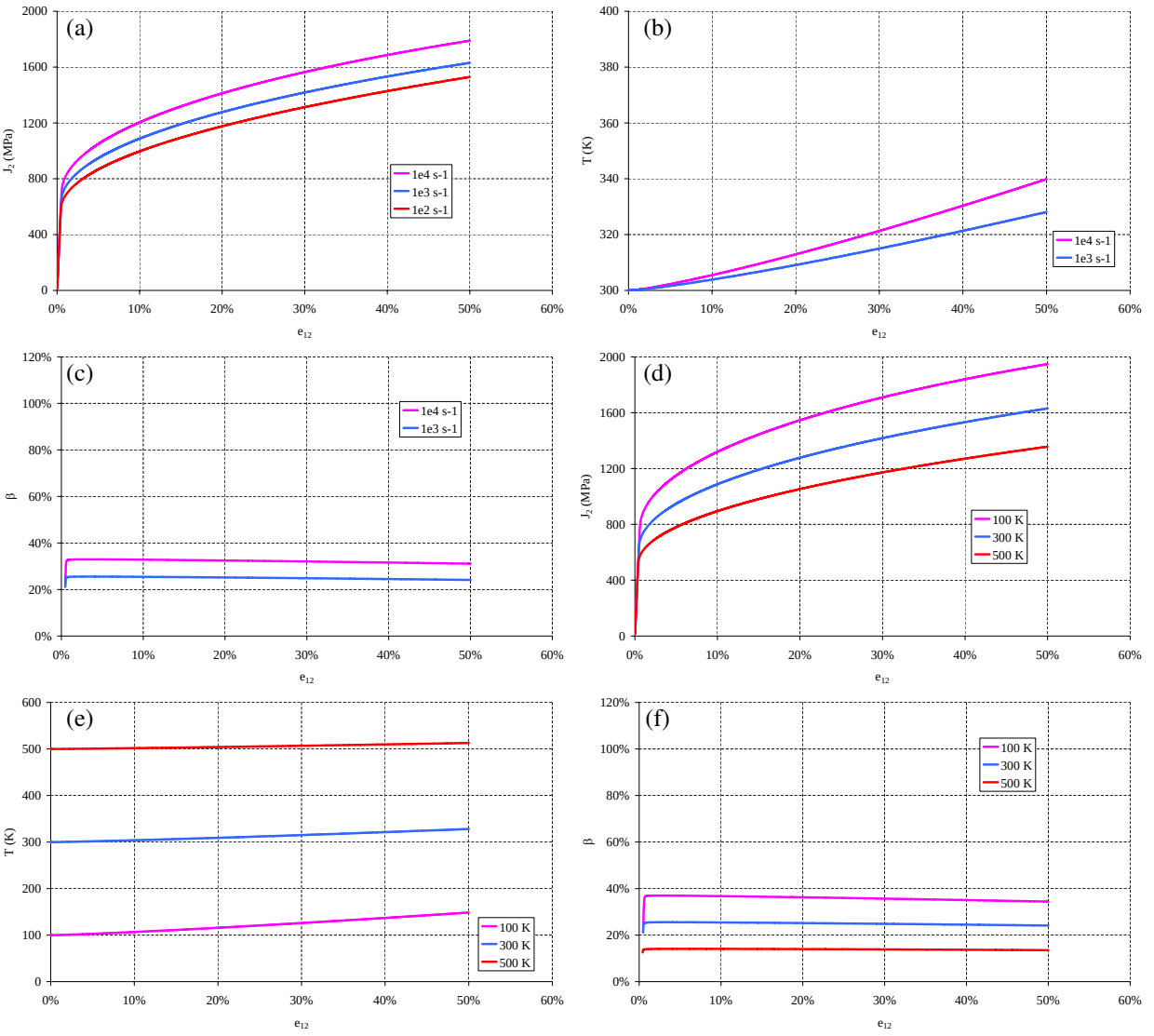

Figure 2. Influence of shear strain rate $\dot{\Gamma}$ and initial temperatures T_0 on stress invariant, heating and inelastic heat fraction for the HMLRO-FE-MUL-NYS hardening model: (a) stress invariant J_2 versus strain e_{12}, with $T_0 = 300\,\mathrm{K}$; (b) temperature T versus strain e_{12}, with $T_0 = 300\,\mathrm{K}$; (c) inelastic heat fraction β versus strain e_{12}, with $T_0 = 300\,\mathrm{K}$; (d) stress invariant J_2 versus strain e_{12}, with $\dot{\Gamma} = 10^3\,\mathrm{s}^{-1}$; (e) temperature T versus strain e_{12}, with $\dot{\Gamma} = 10^3\,\mathrm{s}^{-1}$; (f) inelastic heat fraction β versus strain e_{12}, with $\dot{\Gamma} = 10^3\,\mathrm{s}^{-1}$.

strain rate (Figure 3b) and lower for higher initial temperature (Figure 3e). At $1000\,\mathrm{s}^{-1}$ and for $T_0 = 300$ K, the maximum value of temperature increase is close to 10 K, which is not significant.

According to Figure 3c–f, the initial value of β is much lower than 1, increasing with increasing strain rate and with decreasing initial temperature. As in the previous case, the rate of β is close to zero (see also Remark 6).

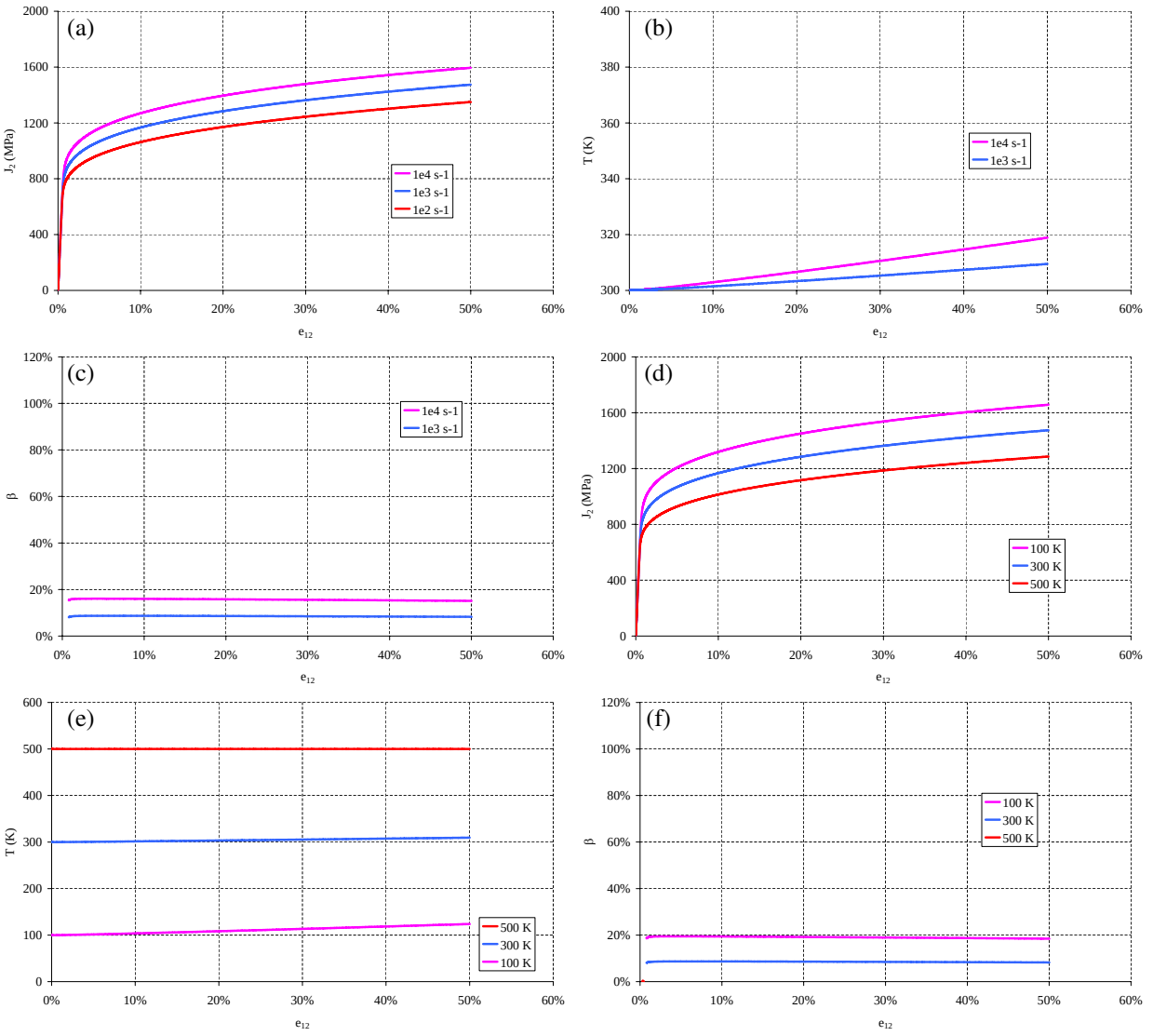

Figure 3. Influence of shear strain rate $\dot{\Gamma}$ and initial temperatures T_0 on stress invariant, heating and inelastic heat fraction for the Johnson–Cook hardening model: (a) stress invariant J_2 versus strain e_{12}, with $T_0 = 300\,\mathrm{K}$; (b) temperature T versus strain e_{12}, with $T_0 = 300\,\mathrm{K}$; (c) inelastic heat fraction β versus strain e_{12}, with $T_0 = 300\,\mathrm{K}$; (d) stress invariant J_2 versus strain e_{12}, with $\dot{\Gamma} = 10^3\,\mathrm{s}^{-1}$; (e) temperature T versus strain e_{12}, with $\dot{\Gamma} = 10^3\,\mathrm{s}^{-1}$; (f) inelastic heat fraction β versus strain e_{12}, with $\dot{\Gamma} = 10^3\,\mathrm{s}^{-1}$.

3.2. ***Strain softening models.*** Consider now the combination HS-FL-ADD-WYS (see Tables 1-4) summarized in Table 9. This combination may correspond to a very high strength (strongly hardened) bcc metal with a linear approximation of temperature dependence (see Figure 4), such as a very high strength martensitic steel or a pure tungsten.

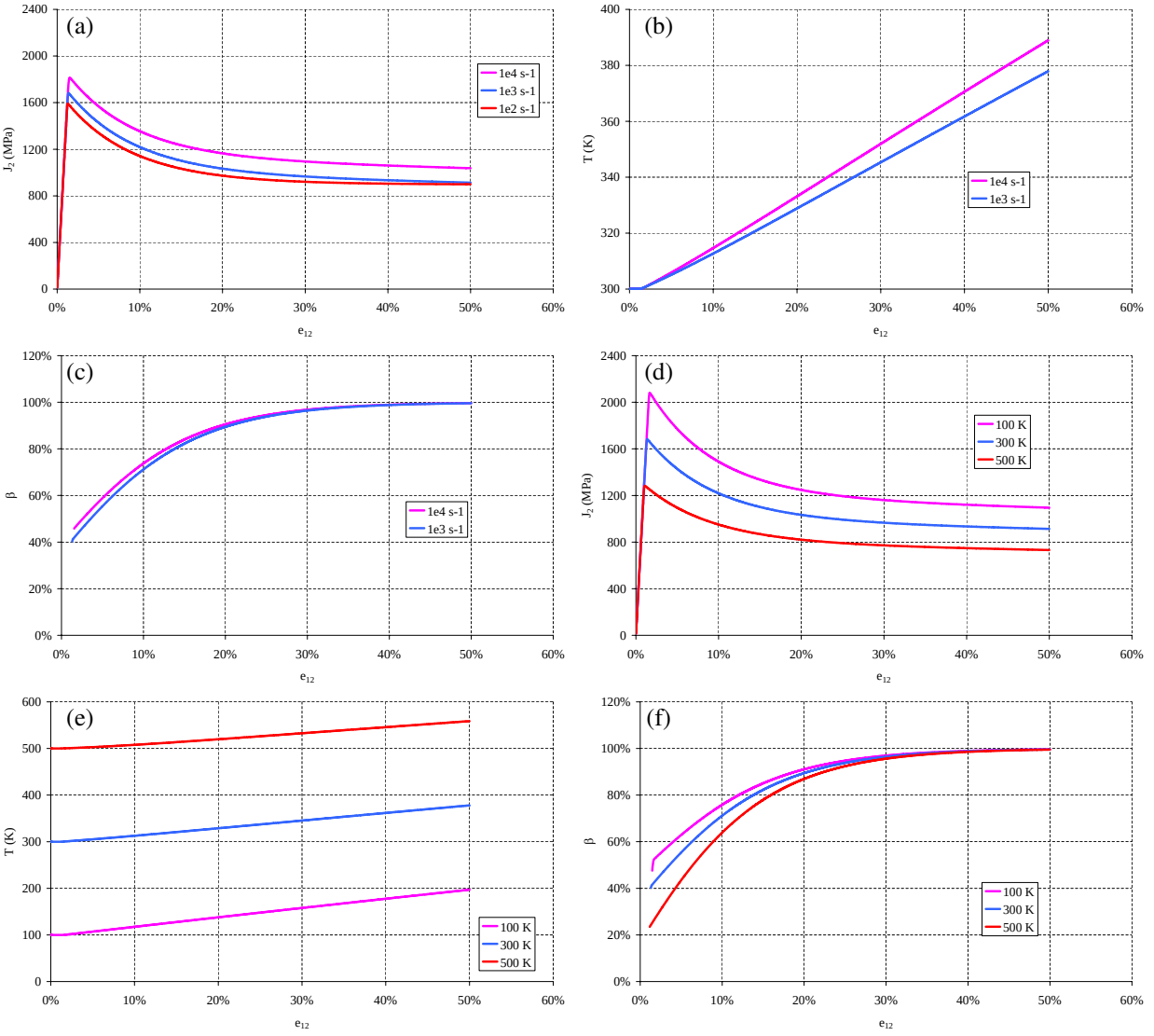

Figure 4. Influence of shear strain rate $\dot{\Gamma}$ and initial temperatures T_0 on stress invariant, heating and inelastic heat fraction for the HS-FL-ADD-WYS softening model: (a) stress invariant J_2 versus strain e_{12}, with $T_0 = 300\,\mathrm{K}$; (b) temperature T versus strain e_{12}, with $T_0 = 300\,\mathrm{K}$; (c) inelastic heat fraction β versus strain e_{12}, with $T_0 = 300\,\mathrm{K}$; (d) stress invariant J_2 versus strain e_{12}, with $\dot{\Gamma} = 10^3\,\mathrm{s}^{-1}$; (e) temperature T versus strain e_{12}, with $\dot{\Gamma} = 10^3\,\mathrm{s}^{-1}$; (f) inelastic heat fraction β versus strain e_{12}, with $\dot{\Gamma} = 10^3\,\mathrm{s}^{-1}$.

Figure 4a shows the thermal softening induced under adiabatic conditions for simulations at plastic strain rates higher than $100\,\mathrm{s}^{-1}$. According to Figure 4b, the temperature rate is higher for higher strain rate while Figure 4e shows that the temperature rate is lower for higher initial temperature. At $1000\,\mathrm{s}^{-1}$ and for $T_0 = 300$ K, the maximal value of temperature increase is close to 80 K.

$h(p)$	$f(T)$	$\Phi(T, p, \dot{p})$	R_0
$-\frac{R_\infty}{k}\exp(-kp)$	$1 - AT$	$Y\dot{p}^{1/m}$	$R_2(1 - AT)$

R_∞ (MPa)	k	$A(K^{-1})$	R_2 (MPa)	Y (MPa s$^{1/m}$)	m
1000	20	10^{-3}	1000	100	6

Table 9. Thermoviscoplastic material constants for HS-FL-ADD-WYS model.

According to Figure 4c–f, the initial value of β is lower than 1, increasing with increasing strain rate and with decreasing initial temperature. The rate of β is positive (according to Remark 3) and its absolute value which is high for small strain tends to 0 for large strain. β tends to unity (100%) for large strain.

Consider finally the combination HMSQ-FL-ADD-WYS (see Tables 1-4) summarized in Table 10. This combination may correspond to a polymer type material (for which the thermomechanical framework used in Section 2 may be applied) with a linear dependence on temperature (see Figure 5).

Figure 5a shows the thermal softening induced under adiabatic conditions for simulations at plastic strain rates higher than $100\,\mathrm{s}^{-1}$. Figure 5b shows that the temperature rate is higher for higher strain rate while Figure 5e shows that the temperature rate is lower for higher initial temperature. At $1000\,\mathrm{s}^{-1}$ and for $T_0 = 300$ K, the maximal value of temperature increase is close to 32 K.

According to Figure 5c–f, the initial value of β is lower than 1, increasing with increasing strain rate and with decreasing initial temperature. The rate of β is initially positive, becomes zero for the minimum of the stress-strain curve (see Figure 5a–d) and becomes negative afterwards (these different stages agree with Remark 3). Its absolute value does not depend on strain rate and on initial temperature at the initial stage (growing β) but depends on initial temperature afterwards.

3.3. ***Summary and complementary analysis.*** In the previous subsection a series of constitutive models involving strain hardening/softening and thermal softening in the context of rate dependent plasticity has been analysed in terms of evolution of stress invariant, temperature and inelastic heat fraction determined from the heat equation under adiabatic constraint.

The first comment concerns the tendency deduced from Remark 2: for a strain hardening model, the inelastic heat fraction decreases with increasing plastic deformation. This tendency has been notably observed experimentally by Lerch et al. [2003] and Jovic et al. [2006] on aluminium alloy and stainless

$h(p)$	$f(T)$	$\Phi(T, p, \dot{p})$	R_0
$-\frac{R_\infty}{k_1}\exp(-k_1 p) + k_2\frac{p^2}{2}$	$1 - AT$	$Y\dot{p}^{1/m}$	$R_2(1 - AT)$

R_∞ (MPa)	k_1	k_2	A (K^{-1})	R_2 (MPa)	Y (MPa s$^{1/m}$)	m
800	60	5000	10^{-3}	500	100	6

Table 10. Thermoviscoplastic material constants for HMSQ-FL-ADD-WYS model.

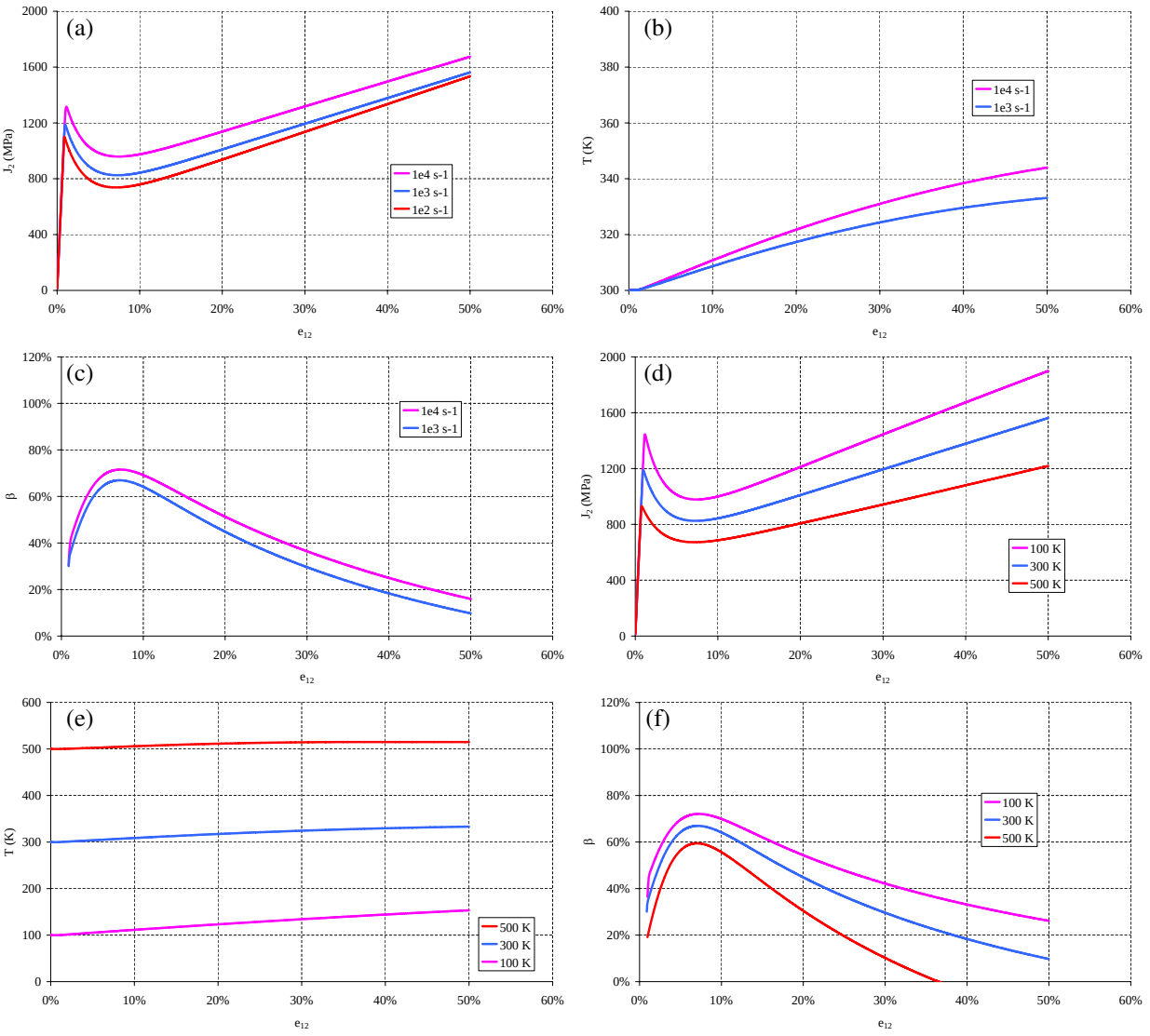

Figure 5. Influence of shear strain rate $\dot{\Gamma}$ and initial temperatures T_0 on stress invariant, heating and inelastic heat fraction for the HMSQ-FL-ADD-WYS softening model. (a) stress invariant J_2 versus strain e_{12}, with $T_0 = 300\,\mathrm{K}$; (b) temperature T versus strain e_{12}, with $T_0 = 300\,\mathrm{K}$; (c) inelastic heat fraction β versus strain e_{12}, with $T_0 = 300\,\mathrm{K}$; (d) stress invariant J_2 versus strain e_{12}, with $\dot{\Gamma} = 10^3\,\mathrm{s}^{-1}$; (e) temperature T versus strain e_{12}, with $\dot{\Gamma} = 10^3\,\mathrm{s}^{-1}$; (f) inelastic heat fraction β versus strain e_{12}, with $\dot{\Gamma} = 10^3\,\mathrm{s}^{-1}$.

steel respectively. The inelastic heat fraction evolution they observe is qualitatively identical to what is obtained numerically herein within the HV-FL-ADD-WYS model (see Figure 1c). Oppositely, according to Remark 2, for a strain softening model the inelastic heat fraction increases and converges to unity. This result (see Figure 4c for HS-FL-ADD-WYS model) can be compared with experimental ones obtained on tungsten by Subhash et al. [1994]. A model combining both strain softening and strain hardening (HMSQ)

allows for an increasing then decreasing inelastic heat fraction. This behaviour is typical of polymeric materials, and the evolution of the inelastic heat fraction obtained numerically for HMSQ-FL-ADD-WYS model (see Figure 5c) reproduces (qualitatively) very well experimental results for polycarbonate [Lerch et al. 2003] and for glassy polymer [Rittel 1999].

The second comment concerns the particular case studied in Remark 5: for a multiplicative rate dependent model (MUL and EXP) combined with the absence of initial yield stress (NYS), the inelastic heat fraction is quasiconstant and its value is very low (see Figure 2b and Figure 3b), leading to weak (and negligible) temperature increase (see Figure 2c and Figure 3c).

On the other hand, for strain hardening models with very similar behaviour, including HV-FL-ADD-WYS, HMLRO-FE-MUL-NYS and Johnson–Cook ones, the maximum value of temperature increase is observed for the former while the minimum value of temperature increase is observed for the latter. Indeed, the corresponding conditions regarding thermomechanical behaviour let in the plastic dissipation induced thermal softening in the first model. On the contrary, this can be hardly reproduced for the Johnson–Cook model. A complete thermodynamics-based approach cannot be applied in this case. This agrees with the experiment-based remark of Chrysochoos et al. [1989] concerning constitutive modelling: some engineering models are not able to reproduce observed phenomena. In order to palliate this deficiency, simplifications are usually done to evaluate temperature growth under adiabatic plasticity conditions. As mentioned previously, they consist (often implicitly), first, in neglecting thermodissipative couplings (see Remark 2) and, second, in considering the inelastic heat fraction as a constant (see Equation (50)). The consequences of these simplifications are now studied.

The heat equation (19) can be decomposed into various contributions. By designating $\dot{Q} = \rho_0 c_0 \dot{T}$, $D = \boldsymbol{\tau} : \boldsymbol{d}^P - R\dot{p} \geq 0$, $\dot{W}^{\boldsymbol{\tau}} = T\dfrac{\partial \boldsymbol{\tau}}{\partial T} : \boldsymbol{d}^{\mathrm{e}}$ and $\dot{W}^R = T\dfrac{\partial R}{\partial T}\dot{p}$, Equation (19) can be rewritten as

$$\dot{Q} = \dot{W}, \quad \text{with } \dot{W} = D + \dot{W}^{\tau} + \dot{W}^R. \tag{33}$$

Three cases are now distinguished depending on the terms retained on the right side of $(33)_{1,2}$.

In the first case, called *quasicomplete heat evaluation*, thermoelastic coupling effects are neglected due to their weak contribution to temperature change: $\dot{W}^{\tau} = 0$. Relation $(33)_2$ is thus reduced to

$$\dot{W} = D + \dot{W}^R = \left[J_2 - \left(R - T\frac{\partial R}{\partial T} \right) \right] \dot{p}. \tag{34}$$

In the second case, the heat equation (20) is further simplified by neglecting both thermoelastic and thermoplastic couplings contributions (see [Voyiadjis and Abed 2006] for a similar simplification). The resulting equation is here called a *simplified heat evaluation*. This means that $\dot{W}^{\boldsymbol{\tau}} = \dot{W}^R = 0$ and $(33)_2$ becomes

$$\dot{W} = D = [J_2 - R]\, \dot{p}. \tag{35}$$

The last case is equivalent to the representation involving a constant inelastic heat fraction β — also known as the Taylor–Quinney coefficient [Mason et al. 1994] — as is frequently done in engineering problems. The resulting equation is here called a *basic heat evaluation*. The expression of work rate $\dot{W}$ in $(33)_2$ in this case reduces to

$$\dot{W} = \beta J_2 \dot{p}. \tag{36}$$

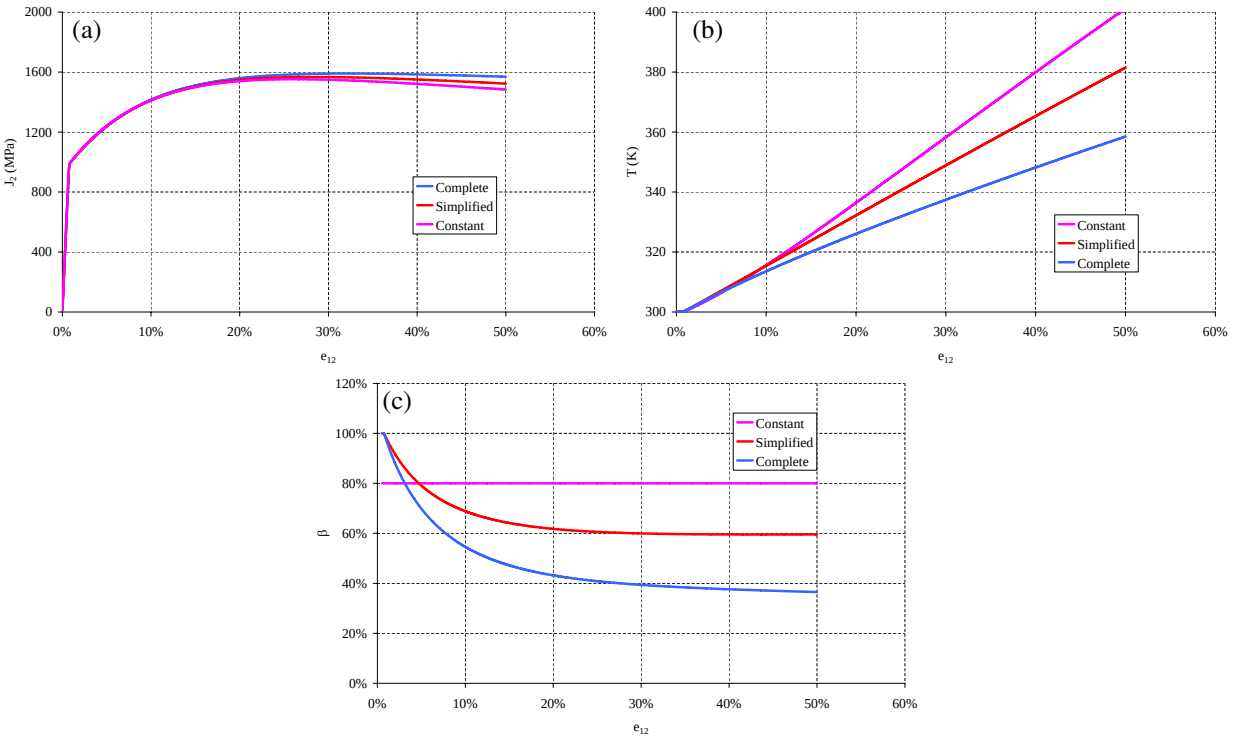

Figure 6. Influence of the simplifications made in the heat equation on stress invariant, heating and inelastic heat fraction considering HV-FL-ADD-WYS hardening model (see Table 6 and Figure 1 for comparison). (a) Stress invariant J_2 versus strain e_{12}; (b) temperature T versus strain e_{12}; (c) inelastic heat fraction β versus strain e_{12}. In each case, $T_0 = 300\,\mathrm{K}$ and $\dot{\Gamma} = 10^3\,\mathrm{s}^{-1}$.

Figures 6–10 show the evolution of the stress invariant, temperature and inelastic heat fraction for a *complete* description, for a *simplified* one and finally, assuming a constant value of the inelastic heat fraction, for the combinations used previously, namely the HV-FL-ADD-WYS type model (Figure 6), the HMLRO-FE-MUL-NYS-type model (Figure 7), the Johnson–Cook model (Figure 8), the HS-FL-ADD-WYS-type model (Figure 9) and the HMSQ-FL-ADD-WYS-type model (Figure 10).

Considering strain hardening models (see Figures 6, 7 and 8), the use of a constant value for β (part c) leads to higher values for temperature (part b) causing a more significant thermal softening (part a). This remark also holds concerning strain hardening/softening model in Figure 10. On the other hand the different methods give very similar results in terms of temperature rates and material behaviour for strain softening model.

4. Effects of heat evaluation method on dynamic plastic localization occurrence

This section aims at showing the influence of the choice of method for evaluating the plastic work-induced heating on the determination of the conditions for dynamic plastic localization onset. The localization phenomenon at stake is adiabatic shear banding (ASB) which constitutes a precursor of

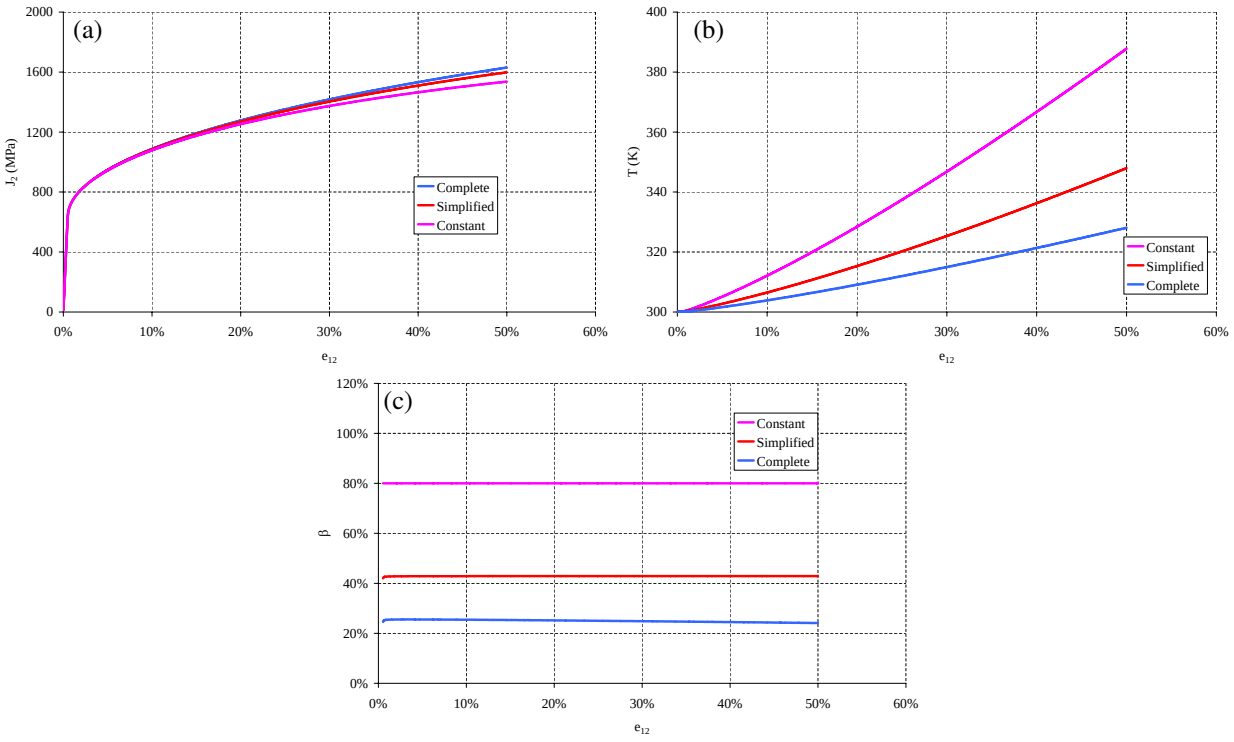

Figure 7. Influence of the simplifications made in the heat equation on stress invariant, heating and inelastic heat fraction considering HMLRO-FE-MUL-NYS hardening model (see Table 7 and Figure 2 for comparison). (a) Stress invariant J_2 versus strain e_{12}; (b) temperature T versus strain e_{12}; (c) inelastic heat fraction β versus strain e_{12}. In each case, $T_0 = 300\,\mathrm{K}$ and $\dot{\Gamma} = 10^3\,\mathrm{s}^{-1}$.

failure of structures submitted to dynamic loading and which intervenes as thermal softening overcomes strain hardening [Marchand and Duffy 1988; Bai and Bodd 1992; Longère et al. 2003].

Conditions for ASB occurrence are commonly obtained from the linear perturbation method which is in general applied in the case of simple shear under constant velocity boundary conditions. Assuming negligible elastic effects, laminar viscoplastic flow and adiabatic conditions, the problem can be reduced to a one-dimensional formulation [Bai 1982; Clifton et al. 1984; Molinari 1985; Batra and Wei 2006] (see e.g. [Anand et al. 1987]) when three-dimensional generalization is presented). Admitting analytical solutions, the linear perturbation method provides in this case a criterion of instability onset, which is interpreted as the incipience of the adiabatic shear banding process, providing in fact the necessary condition for the onset of formation of bands (possibility of a shear band type instability). In the case of ASB phenomena, the extension of the one-dimensional loading criterion to a complex three-dimensional loading can be performed today [Longère et al. 2003]. Simplifications are assumed in order to reproduce qualitatively the different stages of deformation localization (weak and strong) as observed by Marchand and Duffy [1988].

Starting from the governing equations (momentum balance, energy balance, kinematics and constitutive law) in the case of simple shear in a (1, 2)-plane under adiabatic conditions and neglecting elasticity,

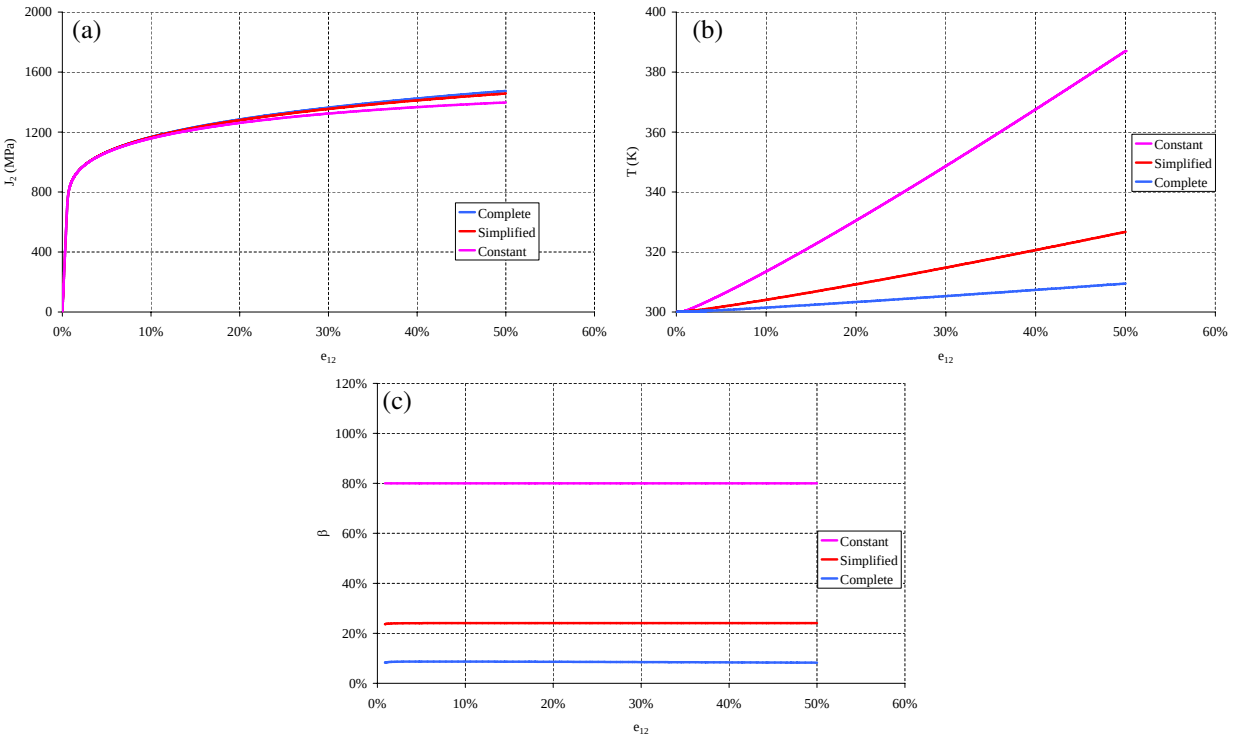

Figure 8. Influence of the simplifications made in the heat equation on stress invariant, heating and inelastic heat fraction considering Johnson–Cook hardening model (see Table 8 and Figure 3 for comparison). (a) Stress invariant J_2 versus strain e_{12}; (b) temperature T versus strain e_{12}; (c) inelastic heat fraction β versus strain e_{12}. In each case, $T_0 = 300\,\mathrm{K}$ and $\dot{\Gamma} = 10^3\,\mathrm{s}^{-1}$.

one obtains the following system:

$$\begin{cases} s_{12,2} = \rho_0 \dot{v}_1, \\ \rho_0 c_0 \dot{T} = \dot{W}, \\ d_{12} = \frac{1}{2}\left(v_{1,2} + v_{2,1}\right) \approx d_{12}^p = \frac{3}{2}\dot{p}\frac{s_{12}}{J_2}, \\ \dot{p} = \Lambda\left(s_{12}, p, T\right). \end{cases} \tag{37}$$

With $J_2 = \sqrt{3}s_{12}$, $v_1 = \dot{\Gamma} x_2$, $v_2 = 0$ and $\Gamma = \dot{\Gamma} t$, the system (37) is reduced to

$$\begin{cases} s_{12,2} - \rho_0 \dot{v}_1 = 0, \\ \rho_0 c_0 \dot{T} - \dot{W} = 0, \\ v_{1,2} - \sqrt{3}\dot{p} = 0, \\ \dot{p} - \Lambda\left(s_{12}, p, T\right) = 0. \end{cases} \tag{38}$$

A small perturbation $\delta U = (\delta v_1, \delta s_{12}, \delta p, \delta T)$ is now superimposed on the set of homogeneous solutions $U = (v_1, s_{12}, p, T)$: $U \Rightarrow U + \delta U$ with $\delta U << U$. Let the perturbation have a wave-like form:

$$\delta U = \overline{U} \exp\left(\varpi t + ikx_2\right) = \overline{U} \exp\left[\varpi_R t\right] \exp\left[ik\left(ct + x_2\right)\right], \tag{39}$$

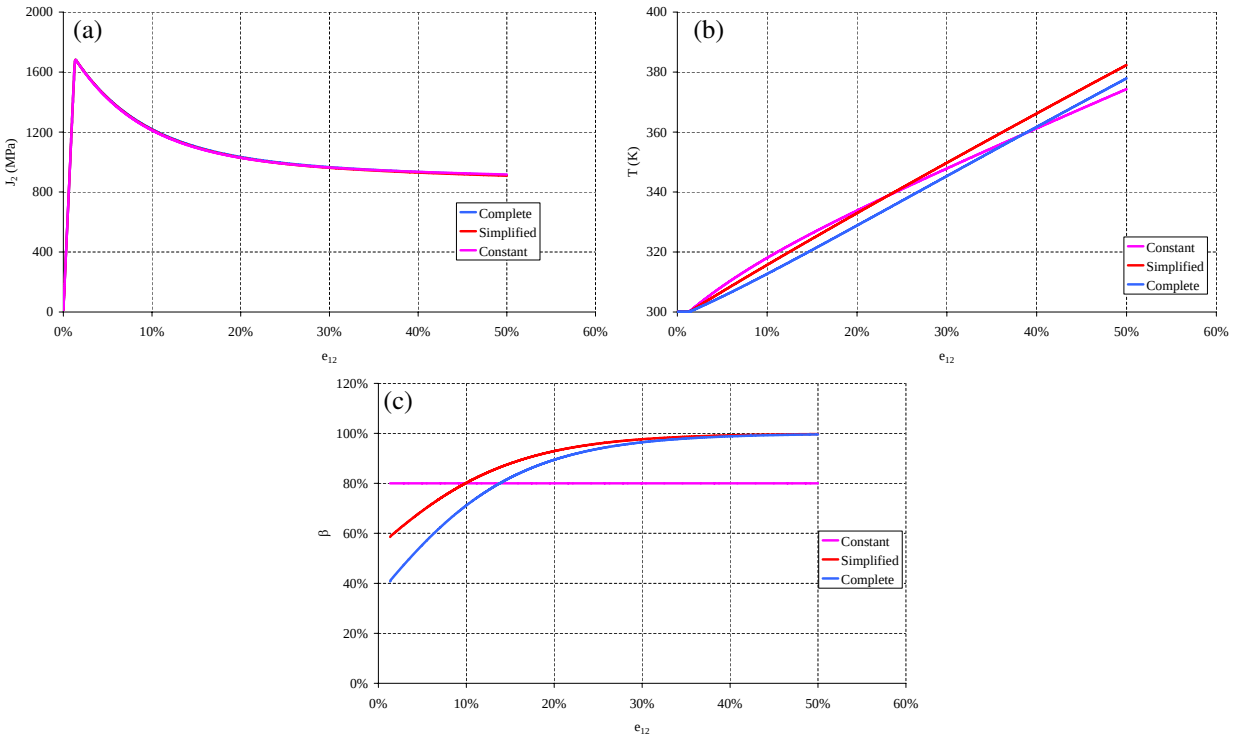

Figure 9. Influence of the simplifications made in the heat equation on stress invariant, heating and inelastic heat fraction considering HS-FL-ADD-WYS hardening model (see Table 9 and Figure 4 for comparison). (a) Stress invariant J_2 versus strain e_{12}; (b) temperature T versus strain e_{12}; (c) inelastic heat fraction β versus strain e_{12}. In each case, $T_0 = 300\,\mathrm{K}$ and $\dot{\Gamma} = 10^3\,\mathrm{s}^{-1}$.

where $\overline{U}$ is the perturbation magnitude, ϖ the wave pulsation, k the wave number, x_2 the wave plane normal, ϖ_R and ϖ_I the real and imaginary parts of the wave pulsation ϖ, and $c = \varpi_I / k$ the wave velocity.

According to the right side of (39), the case $\varpi_R = 0$ points the transition between the stable and unstable states:

(i) if $\varpi_R > 0$, the perturbation may grow with time and the instability mentioned is possible;

(ii) if $\varpi_R < 0$, the perturbation decreases with time.

The objective consists thus in looking for the conditions of the transition from the stable state to the possible unstable state by studying the sign of ϖ_R.

After linearization and using the notations in Table 11 (see next page), the system (38) may be rewritten as follows (see [Longère and Dragon 2007] for further details):

$$\begin{bmatrix} -\rho_0\varpi & ik & 0 & 0 \\ 0 & -w_s & -\left(w_p + w_{\dot{p}}\varpi\right) & \left(\rho_0 c_0 \varpi - w_T\right) \\ ik & 0 & -\sqrt{3}\varpi & 0 \\ 0 & -2P_{12} & (\varpi - B) & -E \end{bmatrix} \begin{Bmatrix} \bar{v}_1 \\ \bar{s}_{12} \\ \bar{p} \\ \bar{T} \end{Bmatrix} = \begin{Bmatrix} 0 \\ 0 \\ 0 \\ 0 \end{Bmatrix}, \tag{40}$$

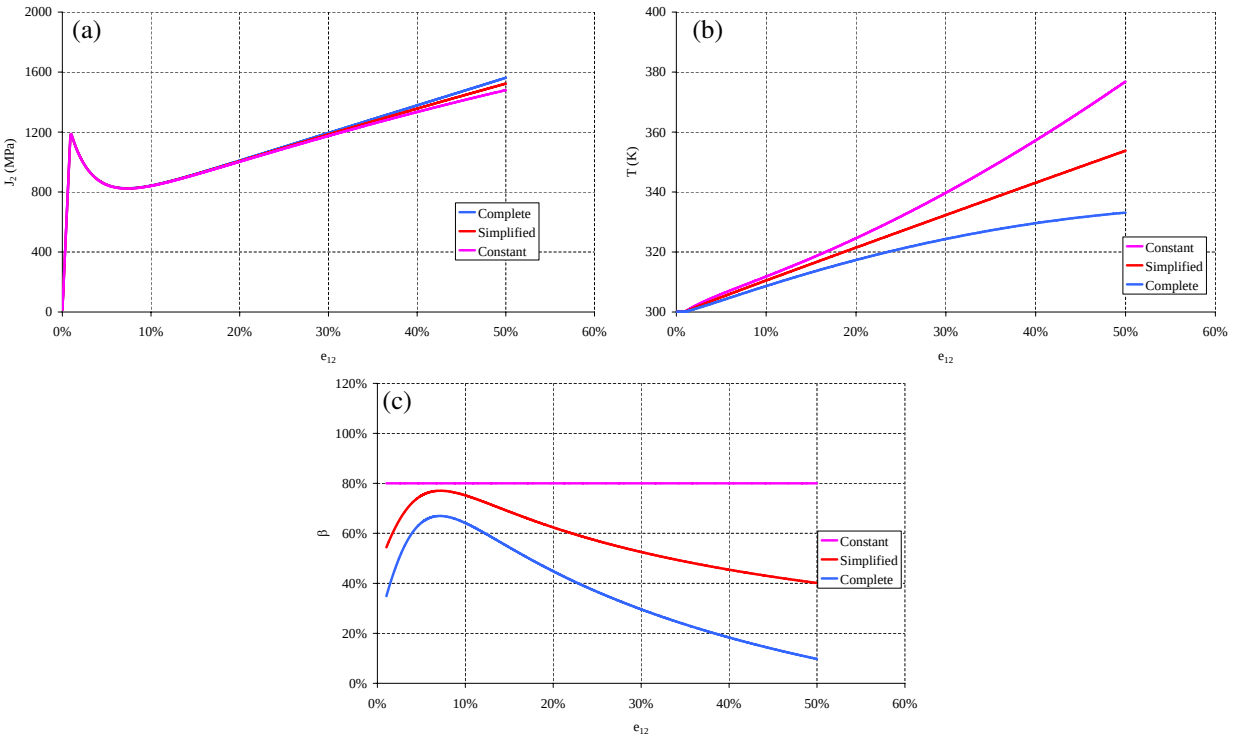

Figure 10. Influence of the simplifications made in the heat equation on stress invariant, heating and inelastic heat fraction considering HMSQ-FL-ADD-WYS hardening model (see Table 10 and Figure 5 for comparison). (a) Stress invariant J_2 versus strain e_{12}; (b) temperature T versus strain e_{12}; (c) inelastic heat fraction β versus strain e_{12}. In each case, $T_0 = 300\,\mathrm{K}$ and $\dot{\Gamma} = 10^3\,\mathrm{s}^{-1}$.

or otherwise:

$$[A]\left\{\bar{U}\right\} = \{0\}\,. \tag{41}$$

The determinant of the matrix $[A]$ in (41), whose components are denoted a_{ij}, is simply

$$\det[A] = a_{11}a_{22}a_{33}a_{44} - a_{11}a_{42}a_{33}a_{24} + a_{12}a_{31}\left(a_{23}a_{44} - a_{43}a_{24}\right). \tag{42}$$

	Basic	Simplified	Quasicomplete
ωs	$\sqrt{3}\beta\dot{p}$	$\sqrt{3}\dot{p}$	$\sqrt{3}\dot{p}$
ωp	0	$-Q\dot{p}$	$-(Q - TY)\,\dot{p}$
ωT	0	$-S\dot{p}$	$TZ\dot{p}$
$\omega_{\dot{p}}$	$\sqrt{3}\beta s_{12}$	$\sqrt{3}s_{12} - R$	$\sqrt{3}s_{12} - (R - TS)$

Table 11. Expressions of ω_i.

The spectral equation deduced from (41) and (42) is a third-degree polynomial in ϖ:

$$\det[\mathrm{A}] = a_3\varpi^3 + a_2\varpi^2 + a_1\varpi^1 + a_0, \tag{43}$$

with

$$\begin{cases} a_3 = \sqrt{3}\rho_0^2 c_0 2P_{12}, \\ a_2 = \rho_0[k^2 c_0 + \sqrt{3}\,(E w_s - 2P_{12} w_T)], \\ a_1 = -k^2\left(E w_{\dot{p}} + w_T + \rho_0 c_0 B\right), \\ a_0 = k^2\left(B w_T - E w_p\right), \end{cases} \tag{44}$$

where

$$P_{ij} = \frac{3}{2}\bar{\alpha}\frac{s_{ij}}{J_2}, \qquad B = -\bar{\alpha}\,Q, \qquad E = -\bar{\alpha}\left[R_0 f'(T) + S\right], \tag{45}$$

$$Q = \frac{\partial R}{\partial p} = h''(p) f(T), \qquad S = \frac{\partial R}{\partial T} = h'(p) f'(T), \qquad \bar{\alpha} = \frac{\partial \Lambda}{\partial F}. \tag{46}$$

As observed by Marchand and Duffy [1988] and demonstrated by Molinari [1985], instability does not imply localization rigorously. Thus the use of the linear perturbation method provides a necessary condition only, leading to a possible *lower* bound for the effective localization incipience. The idea is here to *delay* the instability onset, that is, push it towards an *upper* bound in the sense of approaching the strong localization incipience. In other words we distinguish the *instability point* characterizing locally the equilibrium between strain hardening and thermal softening (maximum of the shear stress-shear strain curve in most cases) and the *localization point* beyond which shear stress drops strongly. The linear perturbation method provides the instability point and we are looking, via a pragmatic engineering evaluation approach, for the localization point which eventually succeeds the instability point.

Adiabatic shear banding occurs as thermal softening overcomes strain hardening. Before the instability point, strain hardening is predominant and the material is necessarily stable, while past the instability point, thermal softening becomes predominant and the material may become unstable. In the linear perturbation method, attenuating thermal softening allows consequently for pushing forward the instability point and approaching the localization point (see [Longère et al. 2003; 2005; Longère and Dragon 2007, for practical applications). Detection of plastic localization onset is essential to control a process of softening behaviour for three-dimensional modelling of thermoelastic/viscoplastic materials incorporating adiabatic shear banding formation and growth.

It is notable that the approximate instability criteria in the sense given above can be applied for any constitutive equations based on irreversible thermodynamics.

As mentioned previously, delaying the strong localization onset with respect to the supposed instability onset is favoured by making $f'(T)$ vanish in the linear perturbation method (concept of 'upper' bound approximation). This approach is consequently used in the following.

Employing Table 11, when considering the basic evaluation, the coefficients a_0–a_3 in (44) become

$$\begin{cases} a_3 = \sqrt{3}\rho_0^2 c_0 2P_{12}, \\ a_2 = \rho_0[k^2 c_0 + 3E\beta\dot{p}], \\ a_1 = -k^2\left(E\sqrt{3}\beta s_{12} + \rho_0 c_0 B\right), \\ a_0 = 0. \end{cases} \tag{47}$$

The spectral equation is, in this case, indeed reduced to a second-degree polynomial in ϖ and $\varpi > 0$ if and only if $a_1 a_3 < 0$. Accordingly, the condition for possible perturbation growth (instability occurrence) is

$$\sqrt{3} s_{12} > \frac{\rho_0 c_0}{\beta} \frac{(\partial R/\partial p)}{-(\partial R/\partial T)}. \tag{48}$$

According to Table 11, the coefficients a_0 to a_3 in (44) in the simplified evaluation become

$$\begin{cases} a_3 = \sqrt{3}\rho_0^2 c_0 2 P_{12}, \\ a_2 = \rho_0 [k^2 c_0 + 3\dot{p}(E + \frac{2}{\sqrt{3}} P_{12} S)], \\ a_1 = -k^2 [E(\sqrt{3} s_{12} - R) - S\dot{p} + \rho_0 c_0 B], \\ a_0 = k^2 \dot{p}\,(EQ - BS), \end{cases} \tag{49}$$

with $E + \frac{2}{\sqrt{3}} P_{12} S = 0$ and $EQ - BS = 0$.

The corresponding components in (49) are thus expressed by

$$\begin{cases} a_3 = \sqrt{3}\rho_0^2 c_0 2 P_{12}, \\ a_2 = \rho_0 k^2 c_0, \\ a_1 = -k^2 [E(\sqrt{3} s_{12} - R) - S\dot{p} + \rho_0 c_0 B], \\ a_0 = 0. \end{cases} \tag{50}$$

The spectral equation is once more reduced to a second-degree polynomial in ϖ and the condition for perturbation growth is given by

$$\sqrt{3} s_{12} > R - \frac{\dot{p}}{\bar{\alpha}} + \rho_0 c_0 \frac{(\partial R/\partial p)}{-(\partial R/\partial T)}. \tag{51}$$

Following the previous procedure for quasicomplete evaluation gives

$$\begin{cases} a_3 = \sqrt{3}\rho_0^2 c_0 2 P_{12}, \\ a_2 = \rho_0 [k^2 c_0 + 3\dot{p}(E - \frac{2}{\sqrt{3}} P_{12} T Z)], \\ a_1 = -k^2 (E[\sqrt{3} s_{12} - (R - TS)] + TZ\dot{p} + \rho_0 c_0 B), \\ a_0 = k^2 \dot{p}[EQ - T(EY - BZ)]. \end{cases} \tag{52}$$

The spectral equation remains a third-degree polynomial in ϖ for which the condition of instability onset is not trivial. In order to obtain a practical criterion in the sense of [Bai 1982], the condition for instability onset is again deduced from the sign of the product $a_1 a_3$.

The condition for perturbation growth in this case is given by

$$\sqrt{3} s_{12} > R - T\left(\frac{\partial R}{\partial T} - \frac{(\partial^2 R/\partial T^2)}{(\partial R/\partial T)} \frac{\dot{p}}{\bar{\alpha}}\right) + \rho_0 c_0 \frac{(\partial R/\partial p)}{-(\partial R/\partial T)}.$$

The conditions for dynamic plastic localization occurrence for the basic heat evaluation method, the simplified heat evaluation method and the quasicomplete heat evaluation method, as defined above, are

$$\sqrt{3} s_{12} > \frac{\rho_0 c_0}{\beta} \frac{(\partial R/\partial p)}{-(\partial R/\partial T)}, \qquad \sqrt{3} s_{12} > R - \frac{\dot{p}}{\bar{\alpha}} + \rho_0 c_0 \frac{(\partial R/\partial p)}{-(\partial R/\partial T)},$$

$$\sqrt{3}s_{12} > R - T\left(\frac{\partial R}{\partial T} - \frac{(\partial^2 R/\partial T^2)}{(\partial R/\partial T)}\frac{\dot{p}}{\bar{\alpha}}\right) + \rho_0 c_0 \frac{(\partial R/\partial p)}{-(\partial R/\partial T)}.$$

(see [Longère and Dragon 2007]). The description of the postlocalization behaviour is not the purpose of the present paper. But in order to visualize the drop in stress induced by adiabatic shear banding, the ASB deterioration model developed by Longère et al. [2003] has been used. The details regarding numerical calculations and corresponding algorithmic procedure can be found in [Longère et al. 2005].

Figures 11 and 12 give, respectively, the material response to shearing and the temperature evolution for the three cases of heat evaluation (two values for β are given). According to Figure 11, the value of shear strain at localization (critical shear strain) onset is close to 30% for basic evaluation with $\beta = 1.0$, close to 32% for basic evaluation with $\beta = 0.8$, close to 35% for simplified evaluation, and close to 38% for complete evaluation. In parallel, the influence of heat evaluation is shown in Figure 12, which gives the evolution of temperature. According to the basic evaluation temperature increases until a value close to 380 K while according to the quasicomplete evaluation, the maximum of temperature remains under 350 K. This difference of 30 K is enough to provoke a difference of 8% for the estimation of the critical shear strain in the conditions prescribed here.

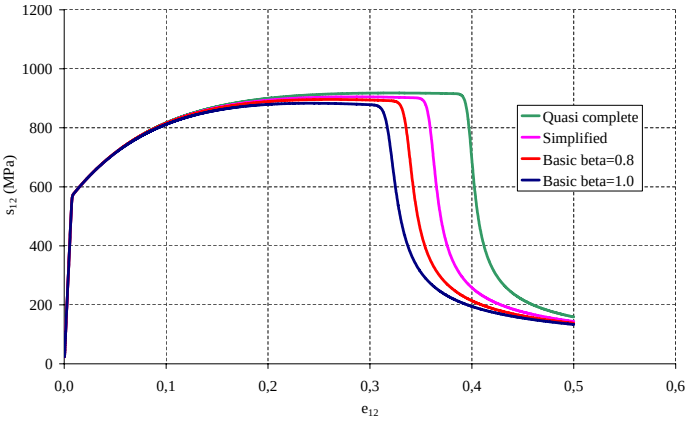

Figure 11. Shear stress versus shear strain: $T_0 = 300$ K; $\dot{\Gamma} = 10^3\ \mathrm{s}^{-1}$.

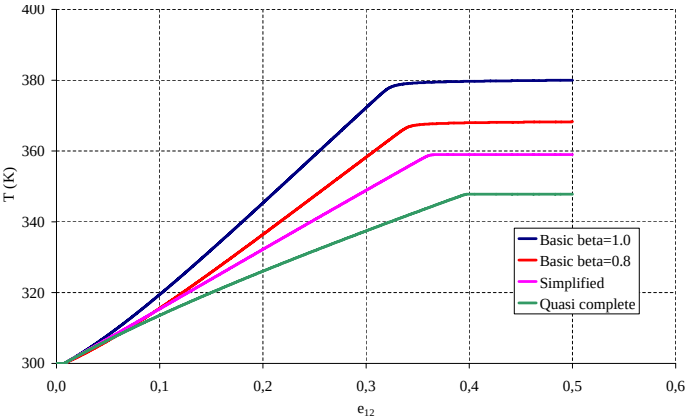

Figure 12. Temperature versus shear strain: $T_0 = 300$ K; $\dot{\Gamma} = 10^3\ \mathrm{s}^{-1}$.

Evaluation type	β	R_0 (MPa)	A (K^{-1})
Basic	1.0	1000	$1.\ 10^{-3}$
	0.8	1015	$1.05\ 10^{-3}$
Simplified	X	1050	$1.1\ 10^{-3}$
Quasicomplete	X	1080	$1.15\ 10^{-3}$

Table 12. Material constants.

In this example, the shear stress-shear strain curves begin to diverge from each other when shear strain is close to 10% (see Figure 11). As a consequence, the value of shear stress at the maximum of each curve is different (the highest is obtained for the quasicomplete evaluation while the lowest is obtained for the basic evaluation for $\beta = 1$). So, we are considering here next shear stress vs. shear strain curves with the same maximum value of shear stress (see Table 12 for the new sets of material constants). Numerical results including instability criterion are given in Figures 13 and 14. In these figures, the values of critical

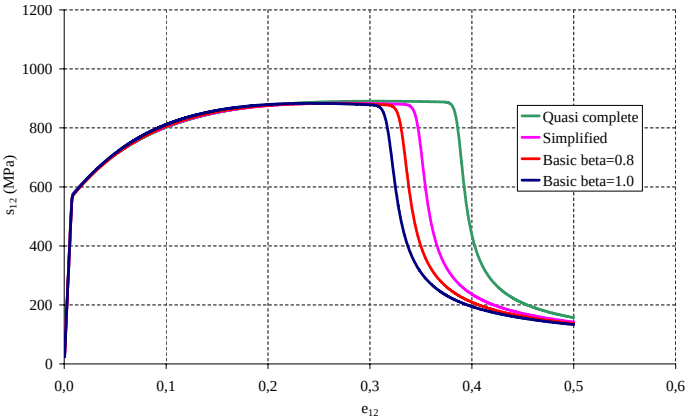

Figure 13. Shear stress versus shear strain: $T_0 = 300\ \text{K}$; $\dot{\Gamma} = 10^3\ \text{s}^{-1}$.

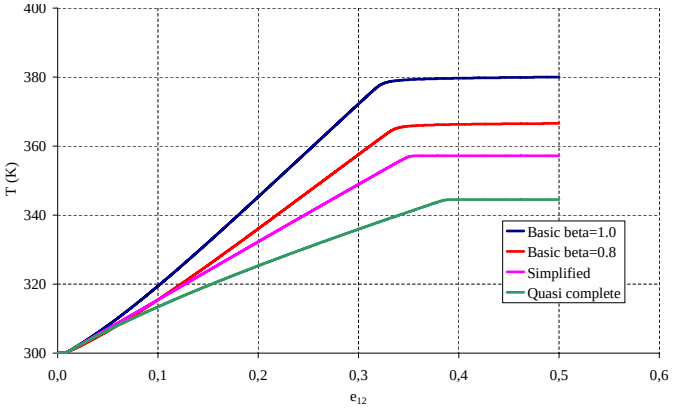

Figure 14. Temperature versus shear strain: $T_0 = 300\,\text{K}$; $\dot{\Gamma} = 10^3\ \text{s}^{-1}$.

shear strain are lower than the previous ones (see Figure 11) but the tendency is preserved: critical shear strain is greater for the quasicomplete evaluation.

5. Concluding remarks

Following an internal variable approach including strain, strain rate and temperature dependence in the context of viscoplastic behaviour embracing a wide range of features involved for a large class of engineering materials, a three-dimensional rather general expression of the evolving inelastic heat fraction has been obtained. This relation allows us to conclude that for a strain hardening model, the inelastic heat fraction decreases for increasing strain, and for a strain softening model the inelastic heat fraction increases and converges to unity. These theoretical results are in agreement with experimental observations. However, depending on the formulation of the constitutive equations, these effects can be well reproduced or totally erased. The choice of the constitutive laws in terms of strain hardening/softening, thermal softening and strain rate dependence is thus crucial. Consequently some models are intrinsically able to reproduce observed phenomena, notably the temperature rise induced by plastic deformation under adiabatic conditions, while others are not. The latter fact sometimes invites selection of an arbitrary, albeit conservative, empirical value for the (constant) inelastic heat fraction. But the use of a constant value for the inelastic heat fraction constitutes a coarse and mostly conservative simplification which can sometimes lead to erroneous results.

The quantitative investigation presented, which employs a spectrum of existing thermoviscoplastic modelling variants at finite strain, aims to show some history effects on the evolution of the inelastic heat fraction β in dynamic plasticity. It points out some limitations regarding commonly employed hypotheses and simplifications concerning the variation of β in engineering applications. It indicates the need for more involved experimental research and for enhanced description of thermomechanical couplings. The multiscale aspects were deliberately set apart in this text, which, in some aspects, provides a critical review of the field while remaining subject to the limits of phenomenological modelling. However, the thermodynamical and physical status of absolute temperature with respect to microscopic heterogeneity of, say, polycrystalline metals and other engineering materials, represents in itself a further challenge and needs more clarification.

References

[Anand et al. 1987] L. Anand, K. H. Kim, and T. G. Shawki, "Onset of shear localization in viscoplastic solids", *J. Mech. Phys. Solids* **35**:4 (1987), 407–429.

[Aravas et al. 1990] N. Aravas, K.-S. Kim, and F. A. Leckie, "On the calculations of the stored energy of cold work", *J. Eng. Mater. Technol.* (*ASME*) **112**:4 (1990), 465–470.

[Bai 1982] Y. L. Bai, "Thermo-plastic instability in simple shear", *J. Mech. Phys. Solids* **30**:4 (1982), 195–207.

[Bai and Bodd 1992] Y. L. Bai and B. Bodd, *Adiabatic shear localization: occurrence, theories, and applications*, Pergamon Press, Oxford, 1992.

[Bataille and Kestin 1975] J. Bataille and J. Kestin, "L'interprétation physique de la thermodynamique rationnelle", *J. Mécanique* **14**:2 (1975), 365–384.

[Batra and Chen 2001] R. C. Batra and L. Chen, "Effect of viscoplastic relations on the instability strain, shear band initiation strain, the strain corresponding to the minimum shear band spacing, and the band width in a thermoviscoplastic material", *Int. J. Plast.* **17**:11 (2001), 1465–1489.

[Batra and Wei 2006] R. C. Batra and Z. G. Wei, "Shear band spacing in thermoviscoplastic materials", *Int. J. Impact Eng.* **32**:6 (2006), 947–967.

[Bever et al. 1973] M. B. Bever, D. L. Holt, and A. L. Titchener, "The stored energy of cold work", *Prog. Mater. Sci.* **17** (1973), 5–177.

[Campagne et al. 2005] L. Campagne, L. Daridon, and S. Ahzi, "A physically based model for dynamic failure in ductile metals", *Mech. Mater.* **37**:8 (2005), 869–886.

[Chrysochoos et al. 1989] A. Chrysochoos, O. Maisonneuve, G. Martin, H. Caumon, and J. C. Chezeaux, "Plastic and dissipated work and stored energy", *Nucl. Eng. Des.* **114**:3 (1989), 323–333.

[Clayton 2005] J. D. Clayton, "Dynamic plasticity and fracture in high density polycrystals: constitutive modelling and numerical simulation", *J. Mech. Phys. Solids* **53**:2 (2005), 261–301.

[Clifton et al. 1984] R. J. Clifton, J. Duffy, K. A. Hartley, and T. G. Shawki, "On critical conditions for shear band formation at high strain rates", *Scr. Metall.* **18**:5 (1984), 443–448.

[Fressengeas and Molinari 1985] C. Fressengeas and A. Molinari, "Inertia and thermal effects on the localization of plastic flow", *Acta Metall. Mater.* **33**:3 (1985), 387–396.

[Guo et al. 2005] Y. B. Guo, Q. Wen, and M. F. Horstemeyer, "An internal state variable plasticity-based approach to determine dynamic loading history effects on material property in manufacturing processes", *Int. J. Mech. Sci.* **47**:9 (2005), 1423–1441.

[Johnson and Cook 1983] G. R. Johnson and W. H. Cook, "A constitutive model and data for metals subjected to large strains, high strain rates and high temperatures", pp. 541–547 in *Proceedings of the Seventh International Symposium on Ballistics* (The Hague, 1983), 1983.

[Jovic et al. 2006] C. Jovic, D. Wagner, P. Hervé, G. Gary, and L. Lazzarotto, "Mechanical behaviour and temperature measurement during dynamic deformation on split Hopkinson bar of 304L stainless steel and 5754 aluminium alloy", *J. Phys.* (*France*) *IV* **134** (2006), 1279–1285.

[Kapoor and Nemat-Nasser 1998] R. Kapoor and S. Nemat-Nasser, "Determination of temperature rise during high strain rate deformation", *Mech. Mater.* **27**:1 (1998), 1–12.

[Lerch et al. 2003] V. Lerch, G. Gary, and P. Hervé, "Thermomechanical properties of polycarbonate under dynamic loading", *J. Phys.* (*France*) *IV* **110** (2003), 159–164.

[Longère and Dragon 2007] P. Longère and A. Dragon, "Adiabatic heat evaluation for dynamic plastic localization", *J. Theor. Appl. Mech.* **45**:2 (2007), 203–223.

[Longère et al. 2003] P. Longère, A. Dragon, H. Trumel, T. de Resseguier, X. Deprince, and E. Petitpas, "Modelling adiabatic shear banding via damage mechanics approach", *Arch. Mech.* **55**:1 (2003), 3–38.

[Longère et al. 2005] P. Longère, A. Dragon, H. Trumel, and X. Deprince, "Adiabatic shear banding-induced degradation in a thermo-elastic/viscoplastic material under dynamic loading", *Int. J. Impact Eng.* **32**:1-4 (2005), 285–320.

[Marchand and Duffy 1988] A. Marchand and J. Duffy, "An experimental study of the formation process of adiabatic shear bands in a structural steel", *J. Mech. Phys. Solids* **36**:3 (1988), 251–283.

[Mason et al. 1994] J. J. Mason, A. J. Rosakis, and G. Ravichandran, "On the strain and strain rate dependence of the fraction of plastic work converted to heat: an experimental study using high speed infrared detectors and the Kolsky bar", *Mech. Mater.* **17**:2-3 (1994), 135–145.

[Molinari 1985] A. Molinari, "Instabilité thermoviscoplastique en cisaillement simple", *J. Mec. Theor. Appl.* **4** (1985), 659–684.

[Oliferuk et al. 2004] W. Oliferuk, M. Maj, and B. Raniecki, "Experimental analysis of energy storage rate components during tensile deformation of polycrystals", *Mater. Sci. Eng. A* **374**:1-2 (2004), 77–81.

[Perzyna 1966] P. Perzyna, "Fundamental problems in viscoplasticity", *Adv. Appl. Mech.* **9** (1966), 243–377.

[Recht 1964] R. F. Recht, "Catastrophic thermoplastic shear", *J. Appl. Mech.* (*Trans. ASME*) **31E** (1964), 189–193.

[Rittel 1999] D. Rittel, "On the conversion of plastic work to heat during high strain rate deformation of glassy polymers", *Mech. Mater.* **31**:2 (1999), 131–139.

[Rosakis et al. 2000] P. Rosakis, A. J. Rosakis, G. Ravichandran, and J. Hodowany, "A thermodynamic internal variable model for the partition of plastic work into heat and stored energy in metals", *J. Mech. Phys. Solids* **48**:3 (2000), 581–607.

[Sidoroff and Dogui 2001] F. Sidoroff and A. Dogui, "Some issues about anisotropic elastic-plastic models at finite strain", *Int. J. Solids Struct.* **38**:52 (2001), 9569–9578.

[Subhash et al. 1994] G. Subhash, Y. J. Lee, and G. Ravichandran, "Plastic deformation of cvd textured tungsten, I: constitutive response", *Acta Metall. Mater.* **42**:1 (1994), 319–330.

[Taylor and Quinney 1934] G. I. Taylor and H. Quinney, "The latent energy remaining in a metal after cold working", *Proc. R. Soc. A* **143**:849 (1934), 307–326.

[Voyiadjis and Abed 2006] G. Z. Voyiadjis and F. H. Abed, "A coupled temperature and strain rate dependent yield function for dynamic deformations of bcc metals", *Int. J. Plast.* **22**:8 (2006), 1398–1431.

[Zehnder 1991] A. T. Zehnder, "A model for the heating due to plastic work", *Mech. Res. Commun.* **18**:1 (1991), 23–28.

[Zener and Hollomon 1944] C. Zener and J. H. Hollomon, "Effect of strain rate upon plastic flow steel", *J. Appl. Phys.* **15**:1 (1944), 22–32.

Received 17 Dec 2007. Revised 29 May 2008. Accepted 19 Jun 2008.

PATRICE LONGÈRE: patrice.longere@univ-ubs.fr
Université Européenne de Bretagne, UBS-LIMATB (EA 4250), Rue de Saint Maudé, BP 92116, 56321 Lorient, France

ANDRÉ DRAGON: andre.dragon@lmpm.ensma.fr
ENSMA-LMPM (UMR CNRS 6617), Téléport 2, 1 avenue Clément Ader, BP 40109, 86961 Futuroscope-Chasseneuil, France